91602
new 82-10

ontario hydro
research division
COMPLIMENTARY COPY
Please Credit Ontario Hydro Research if
Reproduced in Whole or in Part

THE CHARACTERIZATION OF CARBON-14 CONTAINING PARTICULATE MATERIAL FROM THE GAS ANNULUS SYSTEMS OF PICKERING NGS "A" UNITS 1 AND 2 - SUPPLEMENTARY DATA AND FINAL CONCLUSIONS

F.R. Greening
Chemist
Analytical Services Section
Chemical Research Dept

ABSTRACT

Two new samples of active particulate material associated with the retubing operations at Pickering Units 1 and 2 have been characterized with respect to particle size and morphology and chemical and radiochemical composition. One of the samples, a Unit 1 pigtail flow verification filter, contains carbon-14 particulate material mixed with iron oxide and is very similar to the samples characterized in Part 1 of this report. The other sample, a Unit 2 calandria tube protective sleeve or "tophat", has proved to be unique among all the samples investigated to date in that it has readily provided millicurie quantities of a carbon-14 "mesophase" with a distinctive morphology and exceptionally high specific activity (>1 Ci /g). The analytical methods noted in Part 1 have been used to characterize the carbon-14 mesophase as well as the additional instrumental techniques X-ray photoelectron spectrometry, secondary-ion mass spectrometry and pyrolysis mass spectrometry. The carbon-14 mesophase has been shown to contain about 50% carbon-14 in chemical combination with nitrogen, oxygen and hydrogen. The material evolves $^{14}CO_2$, ^{14}CO, NH_3 and N_2 on heating in vacuo. A definitive structure for the material has not been experimentally proven but a nitrogen poly heterocyclic polymeric species is presented as a useful model compound.

job	file	date	report no
31-508-330	833.74	October 1, 1987	86-217-K

91602
new 82-10

ontario hydro
research division

EXECUTIVE SUMMARY

THE CHARACTERIZATION OF CARBON-14 CONTAINING PARTICULATE MATERIAL FROM THE GAS ANNULUS SYSTEMS OF PICKERING NGS "A" UNITS 1 AND 2 - SUPPLEMENTARY DATA AND FINAL CONCLUSIONS

F.R. Greening
Analytical Services Section
Chemical Research Dept

Investigations of a wide variety of carbon-14 containing samples collected during the retubing operations at Pickering NGS "A" between March 1985 and December 1986 have now been completed. Many of the samples included in the study have provided little useful information on the nature of the carbon-14 species due to their limited carbon-14 content or their dilution with other material such as iron oxide. Some samples of airborne material collected during early shock-heating operations on Unit 2 showed a few particles, (referred to as "Christmas trees" at the time), with unusual morphologies but sample limitations precluded detailed investigations of their nature.

In April 1986, a Unit 2 calandria tube protective sleeve or "tophat" was received by Chemical Research and found to be covered with at least 10m Ci of a high specific activity form of carbon-14. Microscopic examination of samples of particulate material from the tophat quickly revealed more details of the unusual dendritic morphology foreshadowed in the shock-heating filter samples. The Unit 2 tophat subsequently proved to be a valuable source of carbon-14 samples and as such has provided a wealth of information on the nature of the carbon-14 containing species produced in the gas annulus systems at Pickering.

Analytical instrumentation available at Chemical Research, such as a Scanning Auger Microprobe, has been used for most of the investigations of carbon-14 containing samples but additional facilities including an X-ray photoelectron spectrometer and a secondary-ion mass spectrometer at the University of Western Ontario, have also been used.

job	file	date	report no
31-508-330	833.74	October 1, 1987	86-217-K

In summary it has been determined that the carbon-14 exists in chemical combination with nitrogen, oxygen and hydrogen in a polymeric "mesophase", a highly structured coral-like mass which may be broken into micron-sized dendritic particles. These particles mix with other particulate matter occurring in the gas annulus system, mainly γ-active corrosion products (e.g. iron and zirconium oxides) and non-metallic debris such as inactive carbon or silica, to form the highly mobile black dust responsible for the contamination problems experienced during re-tubing operations.

The specific activity of the mesophase is typically ~2 Ci/g, equivalent to about 50% carbon-14. The relative amounts of nitrogen, oxygen and hydrogen, constituting the other 50% of the mesophase, are somewhat dependent on the history of the sample. This is especially true of oxygen which forms a surface layer of labile carboxyl groups and is readily lost as $^{14}CO_2$ by moderate heating of the material or exposure to high energy electrons. Self-irradiation of the mesophase, caused by β-decay of the carbon-14, is probably responsible for the slow evolution of $^{14}CO_2$ from the material at room temperature.

The carbon-14 bound in the mesophase is completely and rapidly converted to $^{14}CO_2$ by heating the material in air or oxygen above 750°C. Heating a mesophase sample in the absence of air to temperatures below 1000°C results in the conversion of a maximum of 40% of the available carbon-14 to a mixture of ^{14}CO and $^{14}CO_2$. Mass spectrometry has shown that nitrogen is lost from the mesophase as NH_3 with moderate heating, but as N_2 at high temperatures. To date only traces of other species such as $H^{14}CN$, $^{14}C_2N_2$ or $^{14}CH_3{}^{14}CN$ have been detected in the gas phase pyrolysis products.

While the structure of the polymeric carbon-14 mesophase remains unknown the hypothetical compound $^{14}C_{20}N_{10}O_{10}H_{20}$ with a double-ladder structure may be used as a useful working model. This proposal is based on a consideration of the hot-atom chemistry prevailing in a nitrogen filled gas annulus system and the fact that similar structures have been suggested by other workers for carbon-nitrogen polymers formed in high-energy environments.

At the very least it may be said that the chemical properties which may be predicted for the model compound are remarkably consistent with the observed behaviour of the carbon-14 mesophase. Probably this is all that can be hoped for in the structural elucidation of such an intractable material.

MRB

FRG

91601
new 82-10

ontario hydro
research division

To Dr. D. Mills
Director of Research

THE CHARACTERIZATION OF CARBON-14 CONTAINING PARTICULATE MATERIAL FROM THE GAS ANNULUS SYSTEMS OF PICKERING NGS "A" UNITS 1 AND 2 - SUPPLEMENTARY DATA AND FINAL CONCLUSIONS

F.R. Greening

A report entitled "The Characterization of Carbon-14 Containing Particulate Material from the Gas Annulus Systems of Pickering NGS "A" Units 1 and 2" was issued by Chemical Research in April 1986/1/. Work has now been completed on the characterization of two additional samples associated with the retubing of Pickering Units 1 and 2. This supplementary report documents the results of the analytical investigations of these additional samples and presents final conclusions on the nature of the carbon-14 particulate. The original report (Reference 1) should be consulted for details of analytical procedures and other background information.

1.0 SAMPLE #1S: TWO UNIT 1 PIGTAIL FLOW VERIFICATION FILTERS

Nitrogen gas is fed to the annular space between each pressure and calandria tube by a 304 L stainless steel pipe known as a pigtail. Because these pipes have a relatively narrow bore (3.86 mm ID), it was necessary, after the removal of all the pressure tubes from a Unit, to confirm that the pigtails were not blocked with material from normal reactor operations, e.g. carbon-14 deposits, or debris from retubing operations. Pigtail flow verification was carried out at both the east and west sides of Pickering Units 1 and 2 by measuring the pressure drop across each pigtail with a vacuum pump. Material removed from the pigtails by the pump was collected in small (5 cm long and 3 cm diameter) cartridge type filters which were sent to Chemical Research for analysis; the filter used for the testing of pigtails at the west reactor face of Unit 1 was received in December '85 and the east face filter in March '86.

A large amount of material (~100 mg) was easily removed from the west face flow verification filter. Inspection of the material showed that it consisted mainly of metallic filings and slivers of wood coated or mixed with smaller amounts of black dust. The filings and slivers are undoubtedly debris produced by the extensive retubing operations carried out at the west face. It was deemed inappropriate to carry out any chemical analyses of active material from the west face filter because of the large amounts of extraneous

non-active material present in the sample. Furthermore it was anticipated that the east face flow verification filter would provide a sample relatively free from retubing debris.

The east face filter did indeed prove to contain only a highly beta-active black dust and all the pigtail filter data presented in this report pertain to the east face sample. Gamma spectrometric analysis of the "as-received" east face filter (Table 1.1), compared with a similar analysis of known weights of loose material removed from the filter showed that the filter had trapped approximately 3 mg of active material; it is not known how many pigtails were vacuumed to collect this quantity of dust.

Table 1.1 The Activities of Gamma-Active Radionuclides Identified in the Unit 1 East Face Flow Verification Filter

Radionuclide	Time of Count (4 Mar/86) Activity (nCi)
Mn-54	1.59 ± 0.09
Co-60	34.72 ± 0.25
Zn-65	1.93 ± 0.09
Zr-95	0.22 ± 0.04
Nb-95	0.40 ± 0.04
Ru-106	0.75 ± 0.10
Sn-113	0.15 ± 0.04
Sb-125	2.50 ± 0.12
Cs-137	0.68 ± 0.07
Ce-144	0.21 ± 0.08

Examination of active particulate material from the east face flow verification filter by optical microscopy showed that it contained mainly black or yellowish particles generally less than 25 μm in diameter (Fig. 1.1). Previous results for Pickering gas annulus system deposits have shown that the black particles are either magnetite, Fe_3O_4, or a carbon-14 containing carbonaceous species while the yellowish particles are ferric oxide, Fe_2O_3, or hydrated ferric oxide, FeOOH,/1/. Auger electron analysis of material from the east face filter confirmed the expected identity of the particles.

A weighed portion (0.65 mg) of active material from the east face filter was treated with HCL (10 mL of 8M) in the presence of H_2O_2 (1 mL of 30%). After boiling for 1 hour the solution was passed through a 0.1 μm Nucleopore filter and iron was determined in the filtrate by flame atomic absorption spectrophotometry. Regardless of whether the iron was estimated as Fe_2O_3 or Fe_3O_4 on average of 60 ± 3% of the initial sample weight was found to be attributable to iron oxides.

Energy dispersive X-ray (EDX) analysis of the acid insoluble residue collected on the Nuclepore filter showed no detectable iron but approximately 15 μg of silicon was found presumably in the form of silica, SiO_2. (N.B. EDX analysis does not show the presence of carbon.) Figure 1.2 is an optical micrograph of the insoluble residue on the Nuclepore filter which Auger electron spectrometry confirmed to be mainly particulate carbon.

Approximately 50 μg of active material from the east face filter was ignited in air and the combustion products trapped in Carbosorb. The material lost 27 $\pm$ 2% of its initial weight and 29.7 $\pm$ 0.3 nCi of carbon-14 was found by liquid scintillation counting of the Carbosorb in the trap; this corresponds to a carbon-14 specific activity of 0.59 $\pm$ 0.09 mCi/g of "as-received" material or 2.2 $\pm$ 0.5 mCi/g of carbon, assuming 27% carbon in the sample.

A number of additional experiments have recently been carried out on active material from the east face pigtail flow verification filter which throw further light on the nature of this sample. The experiments were based on the previously reported observation that some samples of the black dust from the Pickering gas annulus systems are attracted to a permanent magnet/Reference 1, page 25/.

By weighing active material from the east face filter with and without the application of a magnetic field and comparing the results with magnetite standards it was found that the sample contains 23 $\pm$ 2% by weight of magnetite, Fe_3O_4. Given the previously determined value for the iron oxide content of the same sample (60%), it follows that 37 $\pm$ 5% of the sample is non-magnetic ferric oxide, Fe_2O_3.

A tabulation of the compositional data on active material from the east face pigtail flow verification filter is given in Table 1.2.

Table 1.2 Composition of Active Material from the East Face Pigtail Flow Verification Filter

Species	Weight %
Carbonaceous	27 $\pm$ 2
Fe_2O_3	37 $\pm$ 5
Fe_3O_4	23 $\pm$ 2
SiO_2	5 $\pm$ 2
Other (by difference)	~ 8

A partial separation of active material from the east face filter into a magnetic and a non-magnetic component has also been carried out by a magnetic

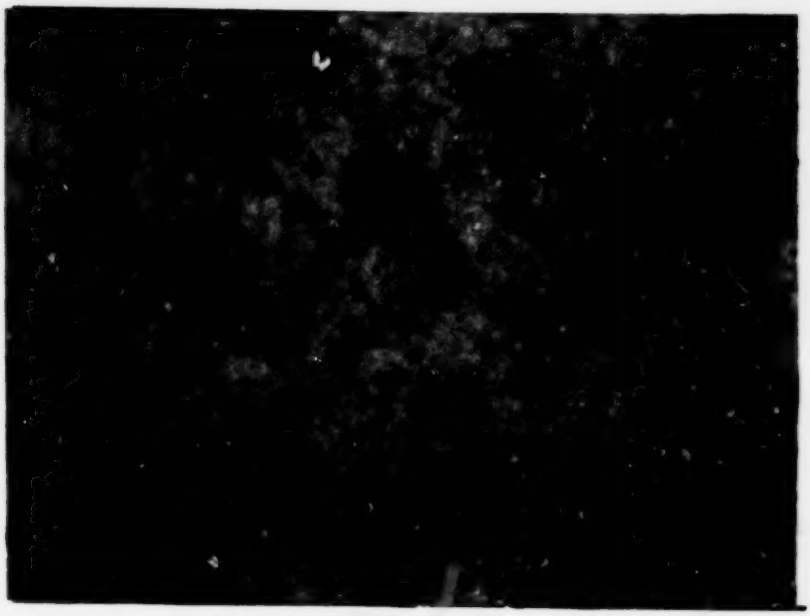

Fig. 1.1 Particles from the East Face Pigtail Flow Verification Filter (Magnification 200X)

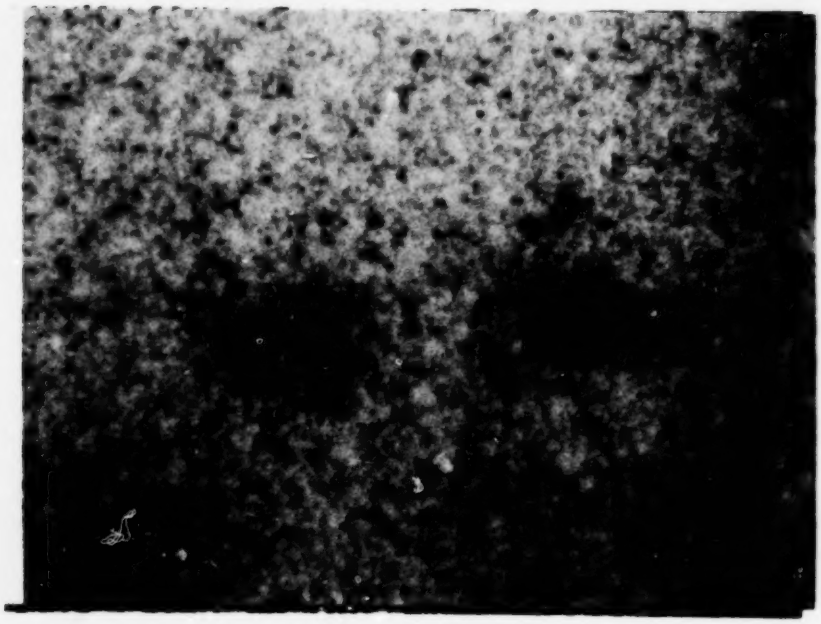

Fig. 1.2 Particles as above After Treatment with HCL/H_2O_2 (Magnification 400X)

filtration technique. It was found that the gamma-active radionuclides are concentrated in the magnetic, magnetite, fraction while the carbon-14 is concentrated in the non-magnetic, ferric oxide, fraction. This observation supports the contention that the magnetite is produced mainly by corrosion within the primary heat transport system and is therefore accompanied by activation products such as Co-60, while the ferric oxide is produced by corrosion within the gas annulus system and is therefore accompanied by carbon-14 (see Reference 1, page 24).

2.0 SAMPLE #2S: A UNIT 2 CALANDRIA TUBE PROTECTIVE SLEEVE OR "TOPHAT"

In the course of the removal of pressure tubes from the Pickering Unit 2 reactor exceptionally high levels of carbon-14 contamination were consistently found on calandria tube protective sleeves (Retubing tools ER-332). These sleeves, usually referred to as "tophats" by virtue of their appearance, function as temporary protective inserts which are positioned at the junction of the lattice and calandria tubes during pressure tube removal. The tophats are used as many times as possible but are discarded when they become excessively damaged which often occurs after insertion in only a few channels.

The very high levels of carbon-14 contamination found on used tophats were usually accompanied by little or no visible deposits. In addition, attempts to decontaminate tophats, even those exposed to only one channel, have been largely unsuccessful.

By the spring of 1986, it was clear that the material contaminating the tophats used in the Pickering Unit 2 vault was a carbon-14 containing species of exceptionally high specific activity. In order to further investigate this material a damaged tophat from the Unit 2 vault was sent to Chemical Research and received April 17 '86. Investigations carried out at Chemical Research on the small amounts of material which may be removed from the surface of the tophat have confirmed that this sample is contaminated with at least 10m Ci of a high specific activity form of carbon-14 which has many remarkable and intriguing properties. There is no doubt that the Unit 2 tophat now at Chemical Research is the most useful source of carbon-14 containing particulate material currently available for investigations of the properties of the Pickering gas annulus deposits. For this reason extensive efforts have been directed at characterizing the carbon-14 removed from this sample. The results of these investigations are presented in the remaining Sections of this report.

2.1 The Morphology of Material from the Unit 2 Tophat

Careful examination of the outside surface of the tophat showed sporadic areas with barely discernible soot-like deposits. Small (5 - 50 μg) amounts of deposit could be transferred from the tophat to indium foils. Observation of these foils by optical microscopy showed the transferred material to consist of black amorphous particles, typically less than 20 μm in diameter, but often agglomerated into groups up to 100 μm across (Figure 2.1). Inspection of the

foils at magnifications up to 1000X (Figure 2.2), also showed the presence of orange-red particles, usually less than 10 μm in diameter, mixed with the black particles. The orange-red particles were typically one-third to one-tenth as abundant as the black particles and were shown by Auger electron analysis to be ferric oxide.

The base of the tophat proved to be an area rich in carbon-14 containing deposits. Material removed from this area consisted mainly of agglomerated black particles and red-brown ferric oxide platelets (Figures 2.3 and 2.4).

It was found that the poor depth-of-field of optical microscopy was severely limiting for the high resolution imaging of these samples. Electron microscopy was therefore used to provide the resolution and depth-of-field needed to reveal the sub-micron features of the tophat deposits. Figure 2.5 is an electron micrograph of the same area of sample as shown optically in Figure 2.3 while Figure 2.6 shows the same area at high magnification.

The black particles in Figure 2.3 appear as bright areas in the electron micrographs, a phenomenon caused by specimen charge buildup. In many cases only a surface layer of adsorbed or labile species is responsible for the poor electrical conductivity of the material and may be eliminated by briefly exposing the specimen to a primary beam current much higher than that normally used for imaging. Figures 2.7 and 2.8 illustrate this effect but show that some damage to the sample may be caused by this treatment.

Residual gas analysis was used to investigate the nature of the desorbed species (see Section 2.3). It was ultimately determined that by careful adjustment of the primary beam current in the range 0.1nA to 10nA, specimen charging and sample damage could both be virtually eliminated.

With optimum beam current selection a survey of the particle morphologies exhibited by tophat deposits was conducted and the results presented in Figures 2.9 to 2.12. It may be seen that agglomerations, up to 100 μm across, of what appear to be partially fused smaller particles, in the range 5 μm to 20 μm, are a common feature of the tophat material. Figures 2.13 to 2.16 show high magnification micrographs of individual particles some of which are up to 20 μm in length and exhibit a characteristic dendritic structure. Clearly these tophat particles are essentially the same as the "Christmas trees" previously observed in a Unit 2 shock-heating filter sample, and reported on page 7 of Reference 1.

2.2 The Radioactivity of Material from the Unit 2 Tophat

Small (5 - 50 μg) samples of tophat deposit were analyzed by gamma spectrometry before and after ignition in air to 1000°C. No losses of gamma-active isotopes were measurable to within the limits of experimental uncertainty for each isotope detected. The resulting specific activities, based on the weights of three ignited residues constituting 40 ± 6% of the initial sample weight, are given in Table 2.1.

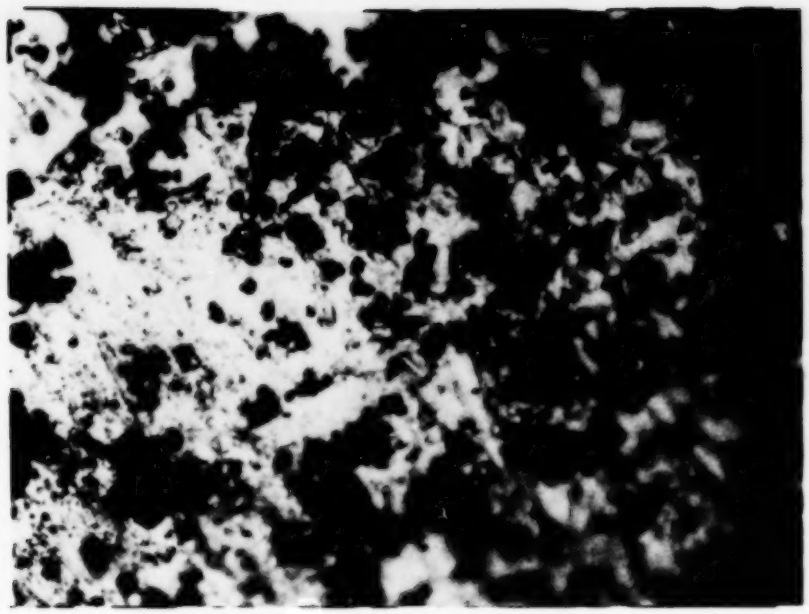

Fig. 2.1 Tophat Deposit (Magnification 400X)

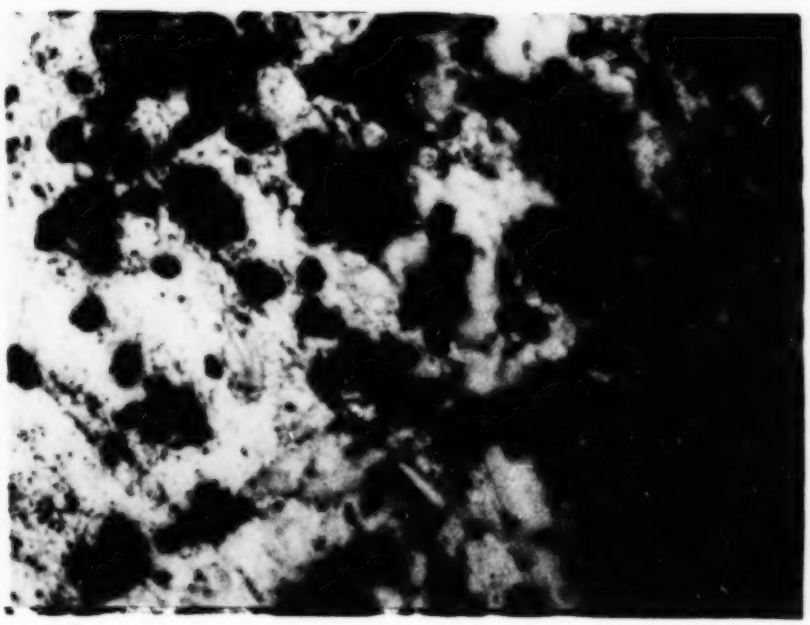

Fig. 2.2 Tophat Deposit (Magnification 800X)

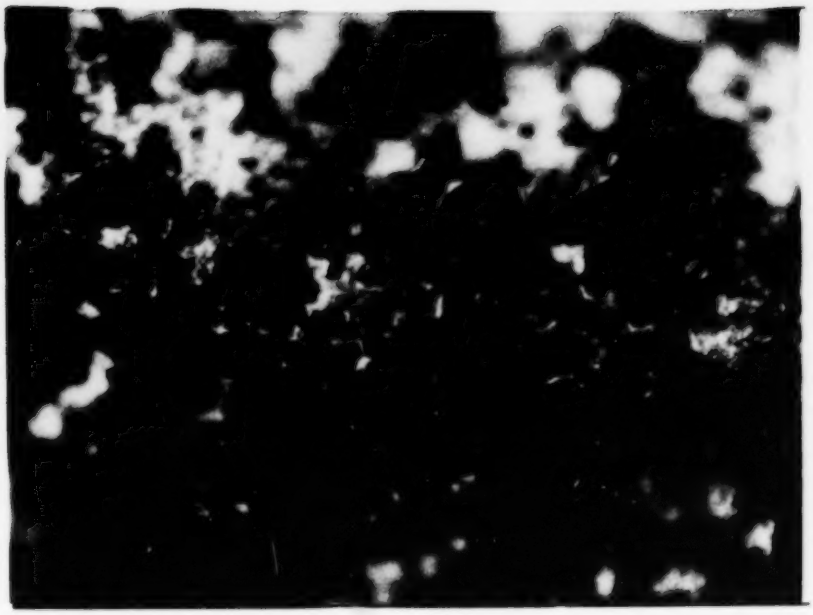

Fig. 2.3 Tophat Deposit Showing Iron Oxide Platelets (Magnification 400X)

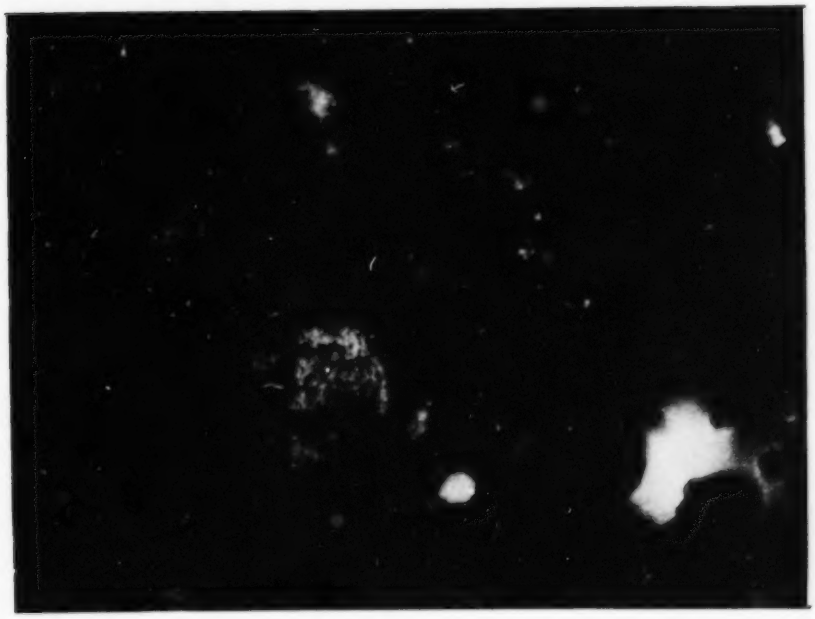

Fig. 2.4 Tophat Deposit Showing Iron Oxide Platelets and Particles (Magnification 800X)

Fig. 2.5 Electron Micrograph of the Tophat Deposit Particles Shown in Fig. 2.3 (Magnification 450X)

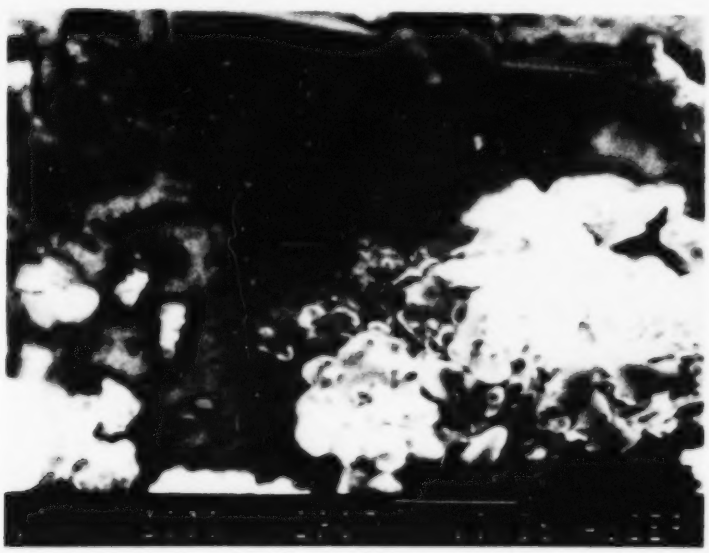

Fig. 2.6 Electron Micrograph of the Tophat Deposit Particles Shown in Fig. 2.3 (Magnification 2000X)

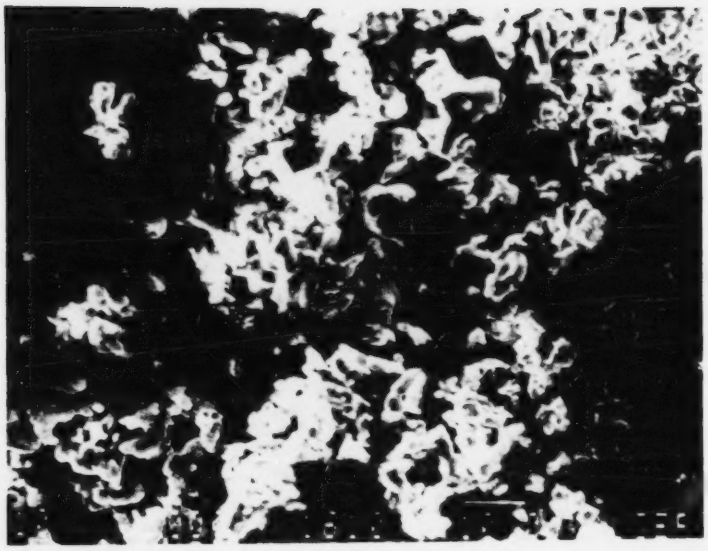

Fig. 2.7 Electron Micrograph of the Tophat Deposit Before Exposure to a High Beam Current (Magnification 1000X)

Fig. 2.8 Electron Micrograph of the Tophat Deposit After Exposure to a High Beam Current (Magnification 1000X)

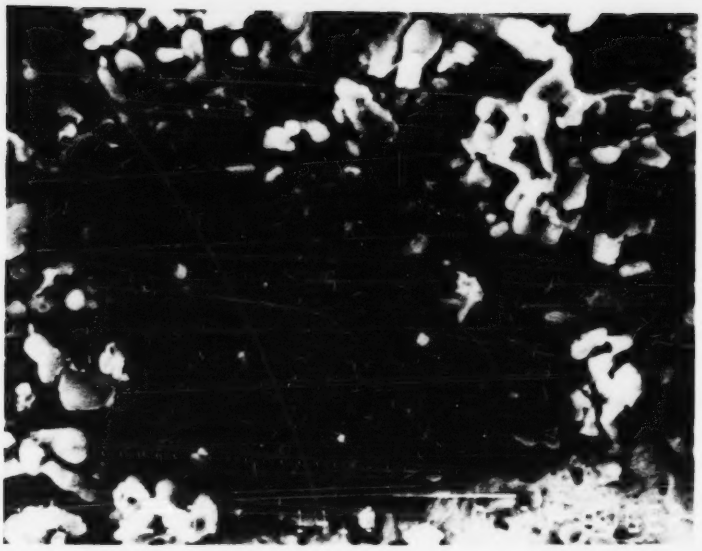

Fig. 2.9 Electron Micrograph of the Tophat Deposit Showing Mainly Iron-Free Material (Magnification 2000X)

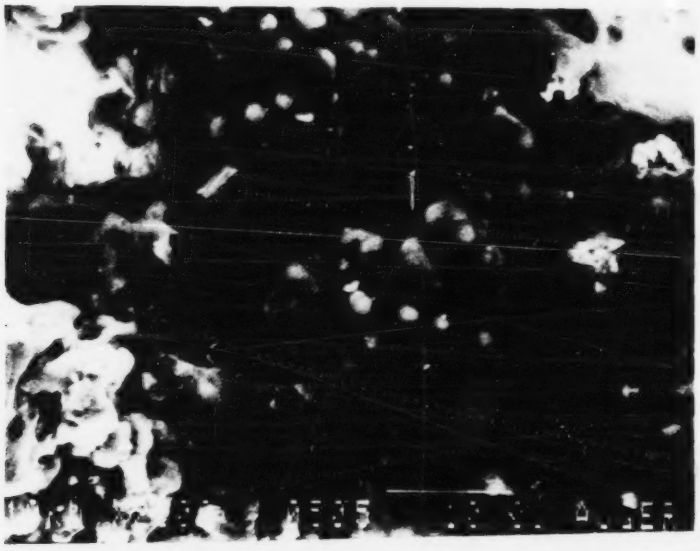

Fig. 2.10 Electron Micrograph of the Tophat Deposit Showing Mainly Iron-Free Material (Magnification 2000X)

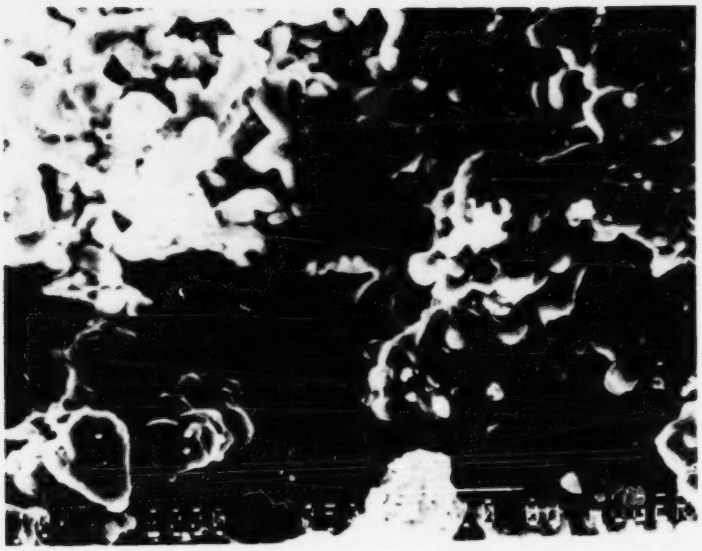

Fig. 2.11 Electron Micrograph of the Tophat Deposit Showing Mainly Iron-Free Material (Magnification 2000X)

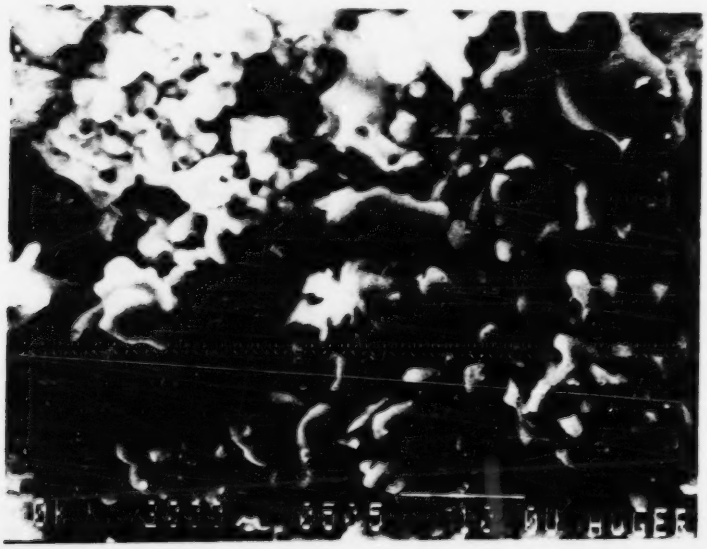

Fig. 2.12 Electron Micrograph of the Tophat Deposit Showing Mainly Iron-Free Material (Magnification 2000X)

Fig. 2.13 Electron Micrograph of the Tophat Deposit Showing Dendritic Particles (Magnification 3000X)

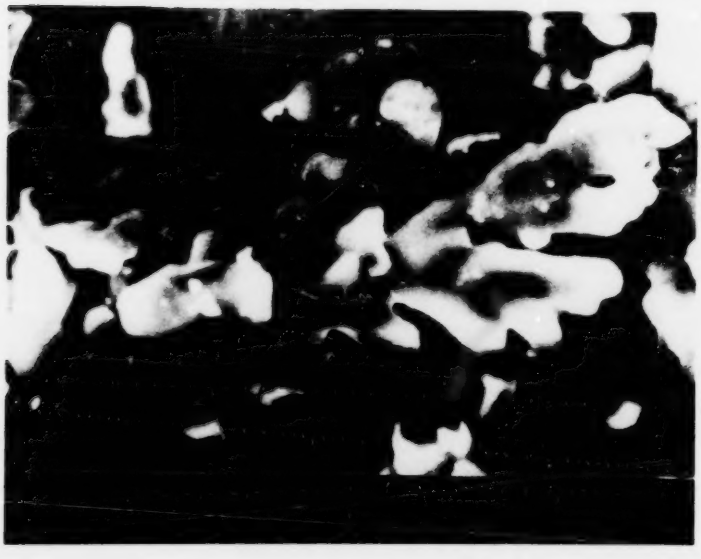

Fig. 2.14 Electron Micrograph of the Tophat Deposit Showing Dendritic Particles (Magnification 4500X)

Fig. 2.15 Electron Micrograph of the Tophat Deposit Showing a Dendritic Particle (Magnification 4500X)

Fig. 2.16 Electron Micrograph of the Tophat Deposit Showing a Dendritic Particle (Magnification 7000X)

Table 2.1 The Average Specific Activity of Gamma-Active Radionuclides Found in Samples Removed from the Unit 2 Tophat

Radionuclide	Specific Activity (nCi/mg)	
	At Time of Count (Sept '86)	At Shutdown (Aug '83)
Mn-54	2.4 ± 0.2	30 ± 3
Co-60	320 ± 10	470 ± 15
Zn-65	14 ± 2	350 ± 50
Nb-94	1.0 ± 0.3	1.0 ± 0.3
Nb-95	0.2 ± 0.1	~40,000
Zr-95	0.1 ± 0.1	~20,000
Ru-106	1 3 ± 0.6	11 ± 5
Sn-113	1.0 ± 0.2	900 ± 200
Sb-125	250 ± 10	560 ± 20
Cs-134	0.9 ± 0.2	2.6 ± 0.6
Cs-137	3.2 ± 0.3	3.4 ± 0.3
Ce-144	0.7 ± 0.3	11 ± 5

Energy depressive X-ray (EDX) analysis of the residues showed them to contain mainly iron, presumably as Fe_2O_3, with smaller amounts of zirconium, chromium, copper, zinc and traces of silicon. An EDX analysis result for a typical residue is given in Table 2.2.

Table 2.2 The Chemical Composition of a Tophat Deposit After Ignition to 1000°C Determined by Energy Dispersive X-Ray Analysis

Element	Weight %
Chromium	1 ± 1
Iron	87 ± 5
Copper	3 ± 1
Zinc	1 ± 1
Zirconium	8 ± 2

The carbon-14 content of a tophat sample was determined by igniting it in a stream of air and passing the effluent gases through two bubblers, the first containing 10 mL of water acidified with 10 mL of 1M HCl and the second containing 20 mL of Carbosorb or 1M NaOH. The first bubbler served to trap any particulate material escaping from the sample during combustion and was invariably found to contain less than 1% of the activity in the second, $^{14}CO_2$

trap. The total activity accumulated in a bubbler was determined by liquid scintillation counting.

The average carbon-14 specific activity determined for three sub-samples of tophat material by the above procedure was 1.1 ± 0.1 Ci/g of initial sample. As noted above, for the sub-samples investigated in this study, the tophat material consists of 40 ± 6% of metal oxides (mainly Fe_2O_3) and 60 ± 10% of a combustible (carbonaceous) component. If a correction is made for the metal oxide content of the tophat material an average carbon-14 specific activity of 1.8 ± 0.4 Ci/g of combustible material is found.

In an additional experiment tophat deposit on an indium foil was subjected to boiling 8M HCl (10 mL) in the presence of 30% H_2O_2 (1 mL) for one hour. The off gases were bubbled through 1M NaOH (20 mL); liquid scintillation counting of this solution verified that no significant loss of carbon-14 had occurred.

Iron was determined in a 5 mL aliquot of the digested sample solution by atomic absorption spectrophotometry after the removal of interfering indium by ion-exchange. Carbon-14 was determined in an additional 1 mL aliquot of the solution by direct liquid scintillation counting. The carbon-14 specific activity determined by this procedure was 0.98 ± 0.05 Ci/g of sample with iron, calculated as Fe_2O_3, constituting 44 ± 4% of the initial sample weight. These results are therefore consistent with those obtained by sample combustion.

2.3 The Chemical Composition of Material from the Unit 2 Tophat

The results discussed above show that the tophat deposit is a mixture of metallic oxides and a carbonaceous species exhibiting a carbon-14 activity of 1.8 ± 0.4 Ci/g. Since 1 g of pure carbon-14 constitutes 4.46 Ci of beta activity, the non-metallic fraction of the tophat deposit must contain 40 ± 9% of carbon-14. The composition of the remaining 60% of the non-metallic component of the tophat deposit has been determined by a variety of techniques including secondary ion mass spectrometry, X-ray photoelectron spectrometry, Auger electron spectrometry and pyrolysis mass spectrometry; the results of these investigations are presented in the remainder of this Section.

2.3.1 Secondary Ion Mass Spectrometry (SIMS) of the Tophat Deposit

Sub-samples of the tophat deposit transferred to indium foils were analyzed by SIMS using the Cameca IMS-3f Ion Microprobe at the Surface Science Laboratory of the University of Western Ontario. Mass spectra were recorded of both the positive and negative secondary ions produced by a 10nA primary beam of Cs^+ ions accelerated to 10 kV and rastered over a 250 μm area of the specimen.

Table 2.3 Positive Secondary Ion Mass Spectral Data from the Tophat Deposit

m/e	Peak Intensity (Counts/s)	Ions
1	1.2×10^2	H^+
2	3.0×10^0	D^+
12	2.0×10^2	$^{12}C^+$
13	1.0×10^1	$^{12}CH^+$
14	1.1×10^3	$^{14}C^+$
15	8.9×10^1	$^{14}CH^+$, $^{14}NH^+$
16	3.8×10^1	$^{16}O^+$, $^{14}NH_2^+$
28	2.1×10^2	$^{14}C_2^+$, $^{28}Si^+$
30	4.7×10^1	$^{14}CO^+$
44	7.9×10^1	$^{12}CO_2^+$
46	3.2×10^2	$^{14}CO_2^+$
52	1.1×10^2	$^{52}Cr^+$
54	8.8×10^1	$^{54}Fe^+$
55	6.1×10^1	$^{55}Mn^+$
56	9.0×10^2	$^{56}Fe^+$
62	7.5×10^1	$^{14}CO_3^+$
63	5.9×10^1	$^{63}Cu^+$
74	1.0×10^2	$^{14}C_3O_2^+$
90	2.0×10^2	$^{90}Zr^+$

Table 2.4 Negative Secondary Ion Mass Spectral Data from the Tophat Deposit

m/e	Peak Intensity (Counts/s)	Ions
1	1.0×10^5	H^-
2	3.1×10^3	D^-
12	1.5×10^5	$^{12}C^-$
13	3.8×10^4	$^{12}CH^-$
14	6.5×10^5	$^{14}C^-$
15	1.6×10^5	$^{14}CH^-$
16	2.5×10^5	$^{14}CH_2$, $^{16}O^-$, NH_2^-
17	7.0×10^4	$^{16}OH^-$
18	2.4×10^3	$^{16}OD^-$
24	7.4×10^4	$^{12}C_2^-$
25	2.9×10^4	$^{12}C_2H^-$
26	1.1×10^6	$^{12}CN^-$, $^{12}C_2H_2^-$, $^{14}C^{12}C^-$
27	2.8×10^5	$^{12}C_2H_3^-$
28	2.6×10^6	$^{14}CN^-$, $^{14}C_2^-$, $^{12}CO^-$
29	4.6×10^5	$H^{14}CN$, $^{14}C_2H^-$
30	2.1×10^4	$^{14}CO^-$, $^{14}C_2H_2^-$
32	1.2×10^4	O_2^-, $^{14}CH_2NH_2^-$
40	8.1×10^4	$^{12}C_3H_4^-$
42	2.1×10^5	$^{14}C_2N^-$, $^{14}C_3^-$, $^{12}CNO^-$
44	7.0×10^4	$^{14}NCO^-$, $^{14}C_2H_2N^-$, $^{14}CN_2H_2^-$
52	3.5×10^4	$^{12}C_4H_4^-$
54	1.4×10^5	$^{12}C_2NO^-$
56	1.8×10^5	$^{14}C_3N^-$, $^{14}C_4^-$, $^{14}C_2N_2^-$

The principal peaks occurring in the positive and negative ion spectra of the tophat deposit are listed in Tables 2.3 and 2.4 respectively. The ion identifications given in the tables are based on comparisons with published SIMS data for carbonaceous materials such as coal or organic polymers./2,3/ In addition the low atomic ion yield of nitrogen relative to carbon has been taken into consideration. For this reason the peak observed at m/e=14 in both the positive and negative ion spectra may be unambiguously assigned to carbon-14 with a negligible contribution from nitrogen-14.

Inspection of Tables 2.3 and 2.4 shows that a large number of molecular species contribute to the tophat deposit spectra especially for negative ions. Unfortunately it is very difficult to determine elemental concentrations from SIMS data of this type due to uncertainties in relative molecular ion yields. Thus the data in Table 2.3 confirms the presence of hydrogen in the tophat deposit but does not allow a H/C ratio to be determined directly. Nonetheless the observed C_nH^-/C_n^- ratios (where C is either ^{12}C or ^{14}C), are comparable to those found for vitrinitic coal for which H/C ~ 5% (W/W)/2/.

For the special case of isotopic ratios, useful information may be extracted directly from SIMS data using the intensities of suitable pairs of peaks. Thus the ion pairs D^+/H^+, D^-/H^- and $^{16}OD^-/^{16}OH^-$ give a consistent value of about 0.03 ± 0.01 for the D/H ratio in the tophat deposit. Similarly the intensity ratios $^{12}C^+/^{14}C^+$, $^{12}C^-/^{14}C^-$ and $^{12}CO_2^+/^{14}CO_2^+$ give a value of 0.22 ± 0.05 for the $^{12}C/^{14}C$ ratio.

2.3.2 X-Ray Photoelectron Spectrometry (XPS) of the Tophat Deposit

X-ray photoelectron spectrometry was carried out on tophat deposits on indium foils using the facilities at the Surface Science Laboratory of the University of Western Ontario. Spectra were excited from a 0.035 mm^2 specimen area using monochromatized AL K_α radiation. The resulting spectra showed peaks attributable to carbon, nitrogen and oxygen with small additional contributions from iron and the indium substrate. A typical spectrum is shown in Figure 2.17.

It was found that the nitrogen (1s) and oxygen (1s) peaks decreased in intensity relative to the carbon (1s) peak by 3% and 2% respectively between successive spectrum scans. This indicates that at least some of the nitrogen and oxygen atoms in the tophat deposit are relatively labile. The fact that the tophat deposit material was formed in the intense radiation field of an operating reactor requires that the material be stable to X-ray irradiation. The observed loss of nitrogen and oxygen during XPS suggests that the tophat deposits have been modified since their removal from the reactor perhaps by partial oxidation.

High resolution scans of the carbon, nitrogen and oxygen 1s peaks were carried out at three randomly selected sample points. In each case broad multiplet peaks spanning up to 6eV were obtained. These multiplets were subjected to a deconvolution procedure and resolved into a set of partially overlapping gaussians. The results of this deconvolution procedure are given in Table 2.5

while Figure 2.18 shows an example of a deconvoluted carbon 1s peak for one of the analysis points. (N.B. The energies reported in Table 2.5 are corrected for a shift of about 4eV due to specimen charging.) Literature data from XPS studies of materials such as organic polymers have been used to make the bonding assignments given in Table 2.5. (See, for example,/4/ and references contained therein.)

2.3.3 Auger Electron Spectrometry (AES) of the Tophat Material

Auger electron spectrometry was carried out on tophat deposits on indium foils using the JAMP-10 Scanning Auger Microprobe at Chemical Research; this instrument allows individual particles down to ~ 1μm in diameter to be imaged and analyzed by an electron beam.

By this technique, it was found that the orange-red particles seen in Figures 2.1-2.4 are ferric oxide, Fe_2O_3, or hydrated ferric oxide, FeOOH, occasionally contaminated with variable amounts of carbon.

Auger spectra of the black particles of the type seen in Figures 2.1-2.4 showed the presence of mainly carbon and nitrogen, (66 ± 6 atomic % and 32 ± 5 atomic %, respectively), with only small amounts of oxygen, (2 ± 1 atomic %), and less than 1 atomic % of iron.

Table 2.5 X-Ray Photoelectron Spectral Data From the Tophat Deposit

Atomic Species	Atomic Concentration (%)	Gaussian Deconvolution Results		
		Centroid Energy (eV)	Relative Contribution (%)	Bonding Environment
Carbon	52 ± 8	284.2 ± 0.1	15 ± 2	N-C-N
		284.8 ± 0.2	24 ± 5	C-C-C
		285.8 ± 0.3	18 ± 3	H_2N-C-C
		286.9 ± 0.3	16 ± 2	N-C-O
		288.0 ± 0.2	12 ± 2	C-C-O
		289.1 ± 0.3	15 ± 3	O-C=O
Nitrogen	22 ± 4	398.2 ± 0.2	39 ± 4	-C-NH_2
		399.2 ± 0.4	33 ± 4	C-N-C
		400.6 ± 0.4	28 ± 6	-N-CO
Oxygen	26 ± 4	531.0 ± 0.3	33 ± 8	C-C-OH
		532.0 ± 0.5	45 ± 8	-C(=O)-O
		533.1 ± 0.5	22 ± 5	N-C-OH

The low levels of oxygen found in the tophat deposit by AES appear to be in conflict with the XPS result reported in Section 2.3.2, where an average of 26 ± 4 atomic % oxygen was found in three sub-samples. It should be emphasized that this discrepancy was completely reproducible even for a sub-sample analyzed initially by AES, which found < 3 atomic % oxygen, and then by XPS, which found ~ 20 atomic % oxygen, and finally by AES, which once again found < 3 atomic % oxygen. A typical Auger spectrum of the tophat deposit is presented in Figure 2.19.

Based on the previous observation of specimen charging effects for low beam currents, i.e. currents below 10nA (see Section 2.1), the question of electron beam damage during AES was investigated/5/. (Beam currents of at least 10nA are required to obtain acceptable signal-to-noise ratios for the acquisition of Auger spectra.) It was found that once a bright, charged, area of a specimen had been discharged by exposure to a 100nA beam, no additional visible changes could be induced in the specimen even by prolonged exposure to currents as high as 1μA. However, the nitrogen KLL peak at 382eV was observed to decrease in intensity by about 20% between successive 100 second spectrum scans, as illustrated in Figure 2.20.

Further evidence for electron beam induced changes to the chemical composition of the tophat deposit was obtained by residual gas analysis of the Auger Microprobe vacuum chamber. The background level of H_2O (m/e = 18) increased substantially after exposing the sample to the electron beam while a small increase in N_2 (m/e = 28) was observed; traces of NH_3 (m/e = 17) and ^{14}CO (m/e = 30) were also detected.

Thus it appears that under electron beam irradiation oxygen is rapidly lost from a surface layer of the tophat deposit, mainly in the form of H_2O, while nitrogen is lost much more slowly, mainly as N_2, from the underlying material; such behaviour allows the results of AES and XPS to be reconciled.

2.3.4 Pyrolysis Mass Spectrometry of the Tophat Deposit

Pyrolysis mass spectrometry of the tophat deposit was carried out on small samples (~ 100μg) loaded into quartz capillary tubes packed with quartz wool. Two different experimental regimes were used both employing the Finnigan 4000 mass spectrometry system at Chemical Research. In one case the sample capillary was inserted directly into the ion source of the mass spectrometer where it could be heated to 350°C. For higher temperatures it was necessary to use an external pyrolysis probe in which the sample could be heated to 1000°C in an inert carrier gas such as helium. In this case the volatile products were taken by a stainless steel line (heated to 200°C) to a jet separator, for the removal of the helium carrier gas, and from there to the mass spectrometer ion source. A disadvantage of this arrangement is the potential for some of the sample pyrolyzates to deposit in the steel line.

For both experimental regimes preliminary measurements were made in which a capillary containing blank quartz wool was taken through the same thermal

Fig. 2.17 X-Ray Photoelectron Spectrum of the Tophat Deposit

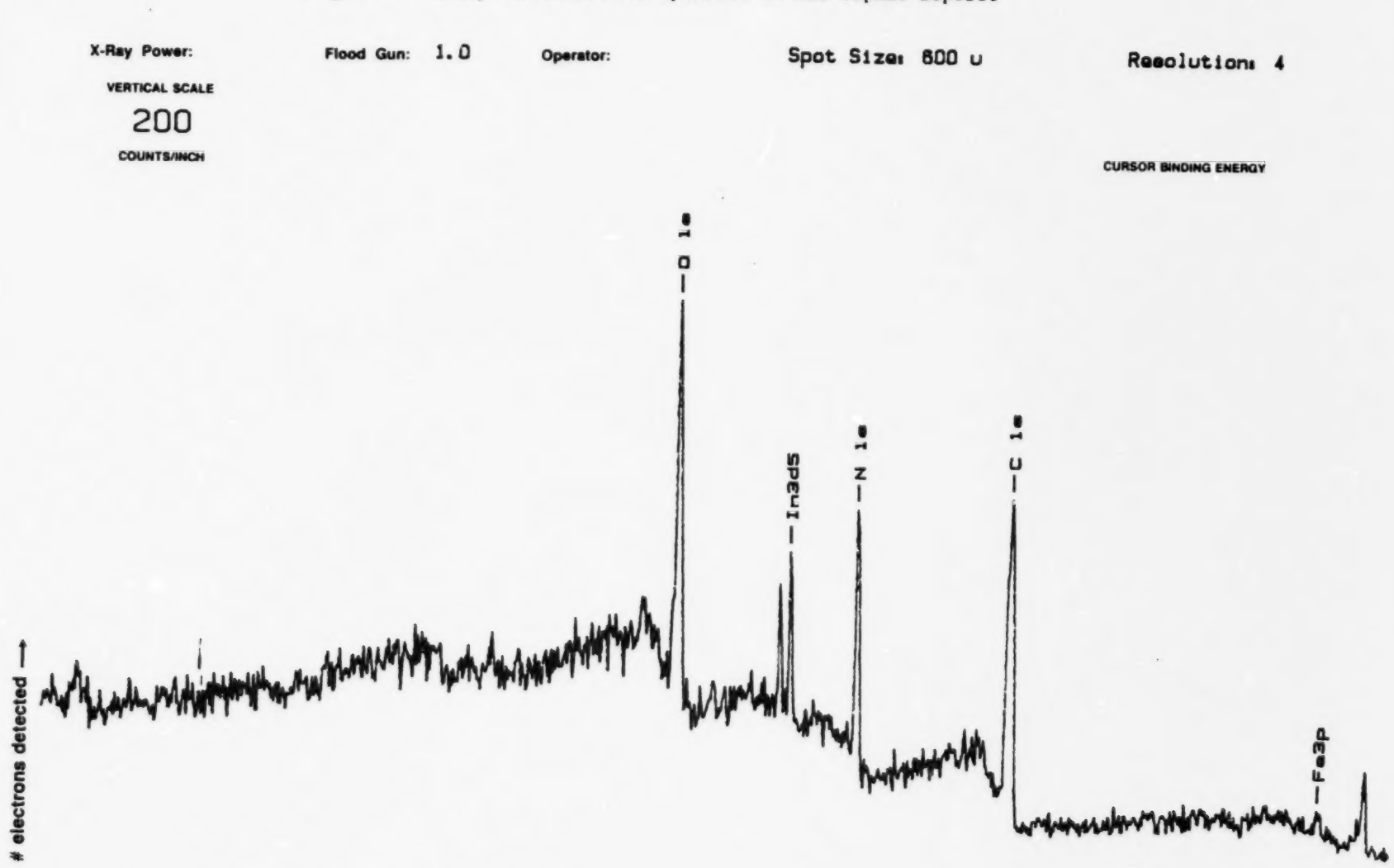

Fig. 2.18 Gaussian Deconvolution of a Carbon 1s Peak in the X-Ray Photoelectron Spectrum of the Tophat Deposit

X-Ray Power: Flood Gun: 1.0 Operator: Spot Size: 800 u Resolution: 2

VERTICAL SCALE

1000

COUNTS/INCH

CURSOR BINDING ENERGY

Energy	Width	Area	%
280.01	1.12	11103	14.8
280.54	1.15	22536	30.0
281.32	1.22	14954	19.9
282.56	1.26	9690	12.9
283.74	1.13	8245	11.0
284.58	1.23	8647	11.5

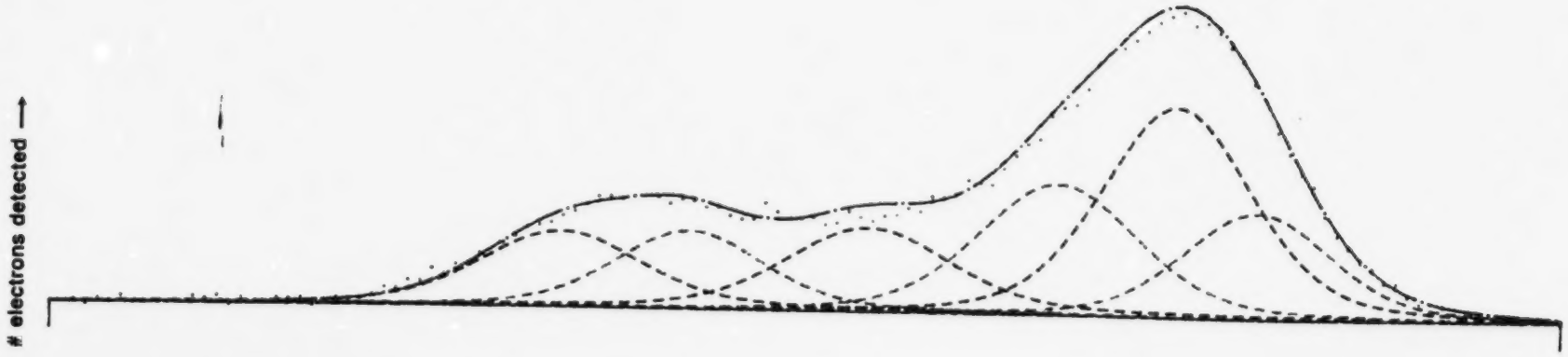

288.0

UPPER BINDING ENERGY (eV)

SAMPLE:

COMMENTS: Disc: HARD

DATE: 9/25/1986

DATA FILE # OH3_02A

← binding energy (eV)

278.0

LOWER BINDING ENERGY (eV)

PICKERING UNIT 2 GAS ANULUS DEPOSIT (TOP HAT)2
OUTSIDE OF TOP HAT C(1S)

9 # SCANS

Surface Science Western

The Surface Science Laboratory, The University of Western Ontario
London, Canada 6A 5B7 (519) 661-2173

OH

Report #:

Spectrum #:

86-217

Fig. 2.19 Auger Electron Spectrum of the Tophat Deposit

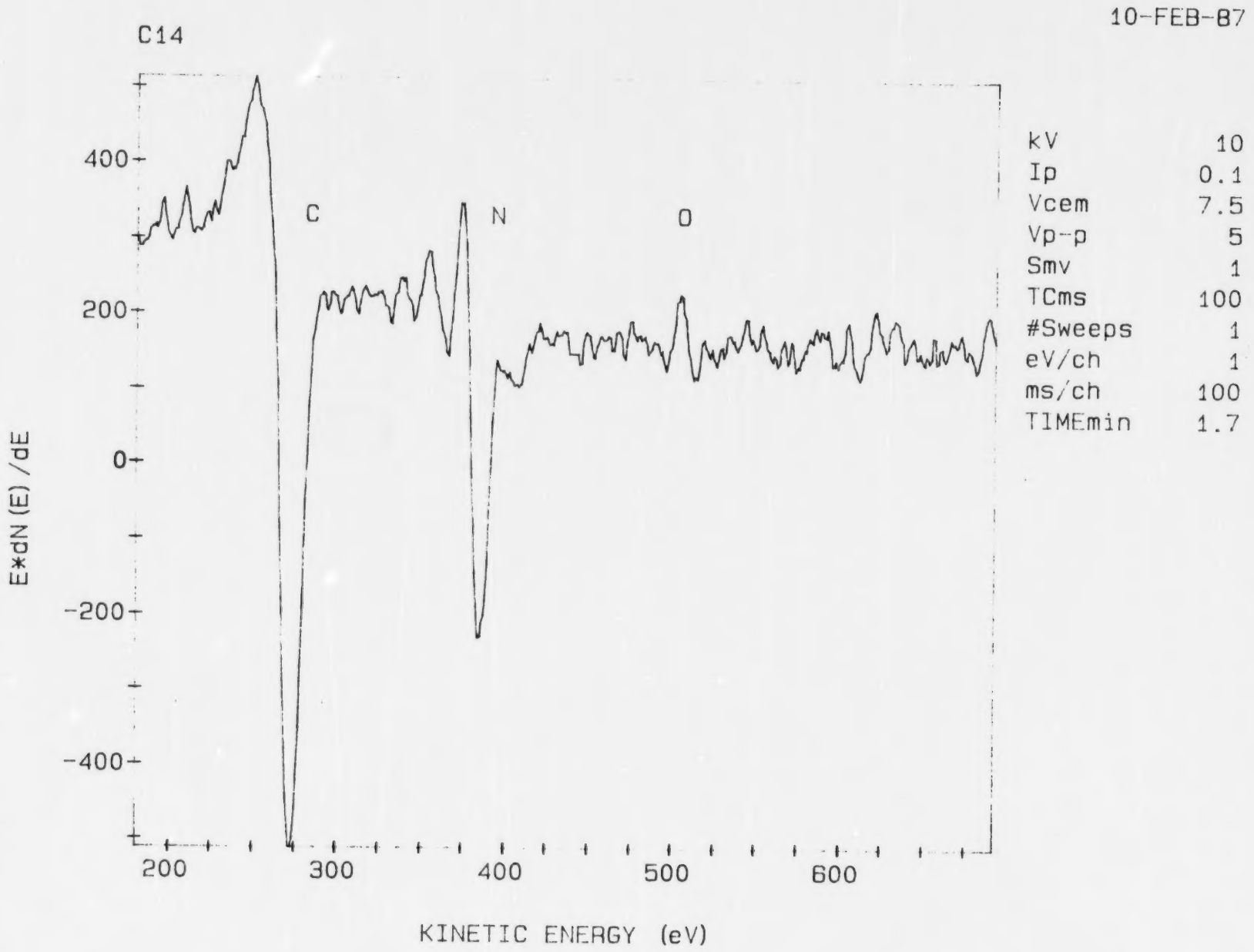

Fig. 2.20 Auger Electron Spectra of the Tophat Deposit Showing the Effect of 100 Second, 100 nA, Electron Beam Exposure

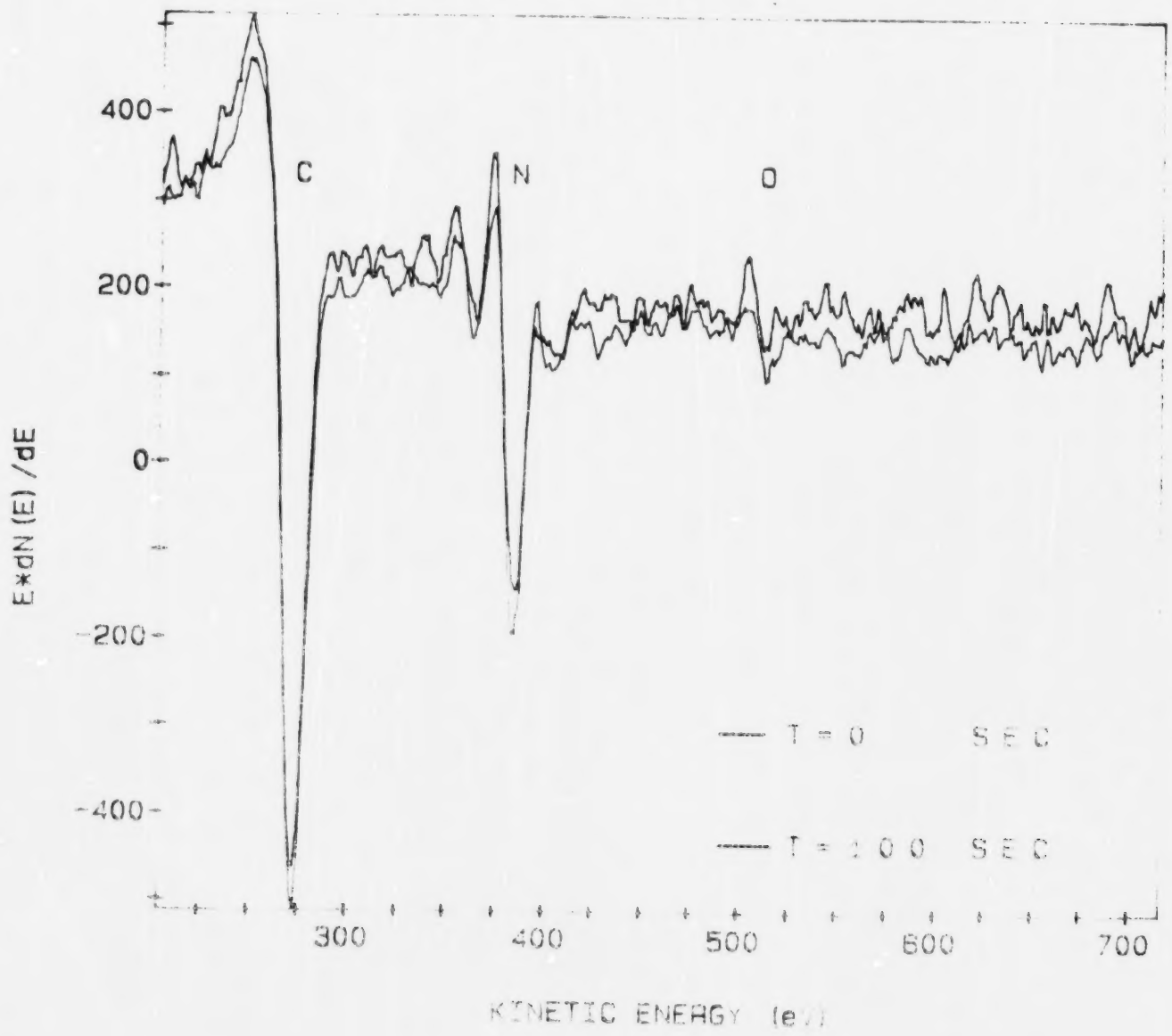

treatment as the sample. The main molecular species released by the blank quartz wool were H_2O (m/e = 18), N_2 (m/e = 28) and $^{12}CO_2$ (m/e = 44). However, the ion counts contributed by these species were generally less than 25% of those contributed by the same species derived from the pyrolysis of the samples.

The results of the pyrolysis of the tophat deposit at temperatures up to 350°C using direct insertion into the ion source are given in Table 2.6. Ion counts from the spectrometer background and blank quartz wool have been subtracted in all cases.

The list of ions presented in Table 2.6 is given without consideration of the relative intensities of secondary peaks reported in mass spectral reference data for pure compounds/6/. If data of this type are taken into account it is readily deduced that the major volatile products resulting from the pyrolysis of the tophat deposit below 350°C are H_2O, NH_3, ^{14}CO and $^{14}CO_2$. (The H_2O possibly stems from the hydrated ferric oxide thought to be present in the sample.) Under the same conditions small but significant amounts of $^{14}CH_3{}^{14}CN$ and $H^{14}CN$ are released while traces of ^{12}C- hydrocarbon contamination are also evident in the pyrolysis products.

The results of the pyrolysis of tophat deposit in the temperature range from 500° to 1000°C are presented in Table 2.7. Data for m/e<20 are not included because of irreproducible, but generally high (~ 10^6 counts), water blanks.

It may be concluded from Table 2.7 that pyrolysis of the tophat deposit at 500°C yields mainly N_2, ^{14}CO and $^{14}CO_2$. It also appears that very little additional decomposition of the tophat deposit occurs at temperatures between 500° and 1000°C.

Table 2.6 Pyrolysis Mass Spectrometry of the Tophat Deposit at 200°C and 350°C by Direction Insertion

m/e	Integrated Peak Intensity (Total Ion Counts)		Ions
	120°C → 200°C	120°C → 350°C	
14	1.3×10^4	1.0×10^5	$^{14}C^+$, N^+
15	1.2×10^4	1.0×10^5	NH^+, $^{14}CH^+$
16	6.6×10^4	7.2×10^5	NH_2^+, $^{14}CH_2^+$
17	1.08×10^5	1.71×10^6	NH_3^+, OH^+, $^{14}CH_3^+$
18	1.08×10^5	3.70×10^6	H_2O^+, $^{14}CH_4^+$
27	2.0×10^4	1.1×10^5	$^{12}C_2H_3^+$
28	2.4×10^4	1.6×10^5	N_2^+, $^{12}CO^+$, $^{14}C_2^+$, $^{14}CN^+$
29	2.8×10^4	1.7×10^5	$H^{14}CN^+$, $^{14}C_2H^+$, $^{12}C_2H_5^+$
30	2.05×10^5	1.38×10^6	$^{14}CO^+$, $^{14}C_2H_2^+$, $^{12}C_2H_6^+$
41	1.3×10^4	1.1×10^5	$^{12}C_3H_5^+$
43	2.2×10^4	1.6×10^5	$^{14}C_2NH^+$, $^{12}C_3H_7^+$
44	1.55×10^5	1.20×10^6	$^{12}CO_2^+$, $^{14}C_2NH_2^+$, $N^{14}CO^+$
45	5.2×10^4	5.0×10^5	$^{14}C_2NH_3^+$, $HN^{14}CO^+$
46	1.21×10^5	1.28×10^6	$^{14}CO_2^+$

The identification of the m/e=30 and m/e=46 peaks as $^{14}CO^+$ and $^{14}CO_2^+$, respectively, has recently been confirmed by a separate experiment in which a tophat deposit sample was heated to 500°C in a stream of nitrogen. The effluent gases were passed through a 0.1M NaOH bubbler, a tube packed with hopcalite, (60% MnO_2 and 40% CuO), heated to 350°C and finally though a second 0.1M NaOH bubbler. The first bubbler served to trap $^{14}CO_2$ while the second bubbler trapped $^{14}CO_2$ derived from the oxidation of ^{14}CO in the heated hopcalite tube. In this way it was found that 7.0 ± 0.5 μCi of $^{14}CO_2$ and 23 ± 2 μCi of ^{14}CO were released from a 100 μg tophat deposit sample, giving a $^{14}CO_2$ to ^{14}CO ratio of 0.30 ± 0.05 in the product gas. The m/e = 46 to m/e = 30 peak ratio observed in the pyrolysis mass spectrometry measurements at 500°C was 0.35 ± 0.01 (see Table 2.7), in good agreement with expectations if these peaks are attributed to $^{14}CO_2^+$ and $^{14}CO^+$ respectively.

Table. 2.7 Pyrolysis Mass Spectrometry of the Tophat Deposit at 500°C and 1000°C in Helium Carrier Gas

m/e	Integrated Peak Intensity (Total Ion Counts)		Ions
	200°C → 500°C	500°C → 1000°C	
28	3.71×10^7	2.2×10^6	$^{14}N_2^+$, $^{12}CO^+$, $^{14}CN^+$
29	8.0×10^5	---	$H^{14}CN^+$
30	3.60×10^7	2.0×10^6	$^{14}CO^+$
44	2.2×10^6	2.0×10^5	$^{12}CO_2^+$
46	1.27×10^7	1.0×10^5	$^{14}CO_2^+$
56	8.0×10^4	---	$^{14}C_2N_2^+$

Inspection of tophat deposit samples after heating in vacuo or an inert gas such as nitrogen or helium has shown that a considerable amount of the initial sample remains apparently unreacted. In fact it is estimated that only 40 ± 10% of the available carbon-14 volatilized below 1000°C. Auger electron analysis of pyrolysed tophat deposit revealed that, apart from the iron oxide particles originally accompanying the carbon-14 containing component of the sample, the carbon remaining in the pyrolysis residue contains no more than 2 atomic % nitrogen and 1 atomic % oxygen.

In concluding this section, it should be noted that samples of tophat deposit slowly release carbon-14 to the ambient air even at room temperature. At least some of the liberated carbon-14 may be trapped in sodium hydroxide solution and is presumably $^{14}CO_2$. In addition some of the released activity is adsorbed on surfaces in close proximity to the sample. Measurements with μCi quantities of tophat deposit sample have shown that the rate of adsorption of emanated carbon-14 by a glass or metal surface decreases to essentially zero over a time period of several days; at the same time the exposed surface approaches a saturation activity of about 1nCi/cm^2.

Because the total amount of carbon-14 released by a tophat deposit sample in a reasonable time interval is very low, e.g. less than 1nCi/day from a 1μCi sample, and the chemical speciation and adsorption/desorption properties of the liberated carbon-14 are not fully characterized, a precise determination of the carbon-14 emanation rate from a tophat sample is very difficult. Measurements have now shown that the emanation rate from a sample is dependent on the cover gas, being greatly reduced in argon or nitrogen; the rate also depends on any pretreatments a sample may have received especially exposure to moist air or volatile solvents.

The best estimates of carbon-14 emanation rates to date have been made using tophat deposit samples sealed with a few grams of askarite in liquid scintillation vials for periods up to 30 days. The total carbon-14 emitted by a sample was taken as the sum of the carbon-14 released by acid distillation of the askarite and the carbon-14 adsorbed on the walls of the vial, determined by direct liquid scintillation counting (carbon-14 released from a tophat deposit as ^{14}CO is, of course, not determined by this procedure). Carbon-14 emanation rates in the range 0.05-0.1%/day have been measured by this procedure using 5-10 μCi tophat deposit samples.

3.0 DISCUSSION

The two samples discussed in this report, namely the pigtail filter debris and the tophat deposit, represent two extremes in the type of carbon-14 containing material found in a nitrogen gas annulus system. The pigtail filter debris has a very low carbon-14 specific activity, ~0.002 Ci/g of combustible material, while the tophat deposit, with a specific activity of about 2 Ci/g of combustible material contains close to 50% carbon-14.

The low carbon-14 concentration in the pigtail debris sample may be attributed to the effects of non-active material diluting the carbon-14 at locations more and more remote from the reactor core. It is significant that the metal oxide contents of the pigtail debris and tophat deposit samples are approximately the same. Evidently a non-metallic/non-active species such as C-12 graphite must be the principal diluent in the pigtail debris sample.

Turning now to the tophat deposit it is probable that this material represents the purest form of solid carbon-14 to be found in a gas annulus system; as such it is a valuable source of information on the chemistry and physics of reactor produced solid carbon-14. The remainder of this Section will be devoted to a discussion of carbon-14 as it appears in the tophat deposit. The discussion will correlate, and hopefully unify, the experimental results presented in the first part of this report.

3.1 Morphology

The micrographs presented in Figures 2.1-2.16 show that carbon-14 occurs in the tophat deposit with morphologies exemplified by the following extreme forms:

(i) Fused masses consisting of anisotropic domains, up to 10 μm in diameter, in an isotropic matrix (see Figures 2.9-2.12).

(ii) Individual dendritic particles, up to 20 μm in length, with rod or leaf-like branches, 1-2 μm in diameter (see Figures 2.13-2.16).

Within this range of morphologies it is difficult, and somewhat meaningless, to define an average particle size. It is possible, however, to envisage particles in the size range 1 μm to 20 μm originating from the tophat deposit.

It has recently been determined by an extensive literature search that the unusual morphology of the tophat deposit is remarkably similar to that exhibited by a carbonaceous material known as "mesophase" produced by the heat treatment of either pure polycyclic aromatic compounds or substances rich in aromatic hydrocarbons such as petroleum or coal-tar pitches/7/. The studies of H. Marsh and co-workers have shown that mesophase is in fact a solidified nematic liquid crystal system whose formation is a consequence of certain essential properties of the precursor molecules. These properties include the occurrence of a laminar structure based on a hexagonal network of carbon atoms as in the graphite lattice. Mesophase precursors also possess the ability to undergo intra and inter-molecular rearrangement and condensation reactions, usually by simple heat treatment, forming polymeric species in the size range 500-1000 amu. The strong dipole interactions between such laminar polymeric units are believed to result in anisotropic domains where discrete particles may eventually coalesce/8/.

It has been reported that compounds with nitrogen and oxygen hetero-atoms in benzenoid rings such as phthalimide, phenazine, etc., promote the formation of mesophase/9/. This result is of particular relevance to the tophat deposit which is known to contain nitrogen, oxygen and hydrogen in addition to carbon-14. It therefore appears that, given its distinctive morphology and favourable chemical composition, the tophat deposit is a carbon-14 rich mesophase consisting of a complex mixture of polymerized heterocyclic species.

3.2 Chemical Composition

The analytical data presented in Section 2 of this report show that the radioactive material removed from the tophat is a mixture of three principal components:

(i) A carbon-14 rich mesophase
(ii) A non-active organic fraction consisting mainly of carbon-12 hydrocarbons
(iii) A γ-active inorganic fraction consisting mainly of iron oxide.

There is now good evidence that both carbon-12 and iron are mixed, rather than chemically combined with the carbon-14 mesophase. Not only is iron found by Auger electron analysis exclusively in oxide particles which are often carbon-free, but variable amounts of iron are measured in relation to carbon-14 during ignition of tophat deposit samples. Experimental uncertainties do not, of course, completely preclude the occurrence of carbon-14 in chemical combination with iron, e.g. as a carbide, but such compounds must constitute minor components, (i.e. less than a few percent), of the tophat deposit.

In the case of carbon-12, SIMS and pyrolysis mass spectrometry data show that the absolute abundances of $C_nH_m^{\pm}$ ions are greater for carbon-12 than for

carbon-14. For all other carbonaceous ions, and in particular for $CO^{\pm}$ and $CO_2^{\pm}$ ions, carbon-14 is more abundant than carbon-12. These results show that the carbon-12 and carbon-14 containing ions are not derived from the same molecular species. It appears that the carbon-12 in the tophat deposit occurs mainly as aliphatic hydrocarbons which probably originate in oil or grease residues on the tophat while the carbon-14 stems from the non-aliphatic mesophase.

If this view is correct and the SIMS derived value of 0.22 is used for the $^{12}C/^{14}C$ ratio (see p. 19), then the carbon-14 specific activity reported in Section 2.2 as 1.8 ± 0.4 Ci/g of carbonaceous tophat deposit becomes 2.3 ± 0.4 Ci/g of mesophase. Since pure carbon-14 has a specific activity of 4.46 Ci/g, mesophase, completely free from metal oxide and inactive carbon, must contain approximately 50% carbon-14 with the remaining 50% being chemically bound hydrogen, nitrogen and oxygen.

Nitrogen and oxygen have been determined directly in the tophat deposit by Auger electron and X-ray photoelectron spectroscopy (AES and XPS). Hydrogen is not detectable by these techniques but its presence may be inferred from the occurrence of species such as $^{14}C_nH_m^{\pm}$ and $NH_n^{\pm}$ in mass spectra derived from the material.

As noted in Section 2.3 of this report, the quantitative results that have been obtained for tophat samples by AES and XPS are somewhat different but may be reconciled by assuming that the surface of the carbon-14 mesophase has been partially oxidized. Surface oxidation of polymers is a well known phenomenon and results in up to a monolayer coverage of the material with carbonyl, carboxyl, ester or lactone groupings/10/; because XPS is highly surface sensitive and relatively non-damaging these species are readily detected by this technique. AES is also highly surface sensitive but more likely to cause specimen damage/4,5/. The much lower abundance of oxygen found in the tophat deposit by AES, (<3%), compared with XPS, (~26%), indicates that the oxy-species noted above are labile under electron beam irradiation.

Electron beam-specimen interactions are a matter of considerable interest for the tophat deposit because the material is continuously exposed to electron irradiation by virtue of its own radioactive decay. It is probable that radiolytically initiated oxidation is at least partially responsible for the emanation of $^{14}CO_2$ from tophat deposit samples stored in air. The extensive literature on the self-decomposition of carbon-14 labelled organic compounds certainly supports this hypothesis and suggests that it may be the dominant decomposition mechanism at room temperature/11/. It is debatable whether self-radiolysis, or electron beam irradiation, of the tophat deposit releases any other species besides $^{14}CO_2$, e.g. $H^{14}CN$. More research is needed to answer this question and to show how the emanation of such species is affected by air, moisture, temperature, etc.

3.3 Molecular Structure

Perhaps the most important, but also the most difficult, question concerning the tophat deposit pertains to its molecular structure. If this were known the properties of the material could be predicted or, alternatively, the carbon-12 analogue could be synthesized and investigated without the restrictions imposed by sample availability, radiation safety, etc.

At present the structure of the carbon-14 component of the tophat deposit remains unknown, if indeed the active material consists of a single molecular species. Information of this type could possibly be provided by diffraction measurements but sample limitations have so far thwarted attempts to use these techniques. None-the-less some structural information on parts of the carbon-14 species, i.e. functional group assignments, have been provided by XPS and mass-spectrometry. It is therefore possible to postulate probable structures for the carbon-14 containing species in the tophat deposit based on such factors as its known chemical composition, number and type of functional groups, and degradation behaviour. It has also been shown that the highest specific activity material in the tophat deposit is a carbon-14 rich mesophase of the type formed by the heat treatment of heterocyclic aromatic species.

Before these experimental data are used to derive potential structures for the carbon-14 mesophase it is useful to first consider the reaction pathways available to nascent carbon-14 in a nitrogen gas annulus system.

It may be calculated that in a Pickering CANDU unit, with about 10^4 litres of nitrogen in the gas annulus system, carbon-14 is produced at a rate of approximately 50g per year mainly by the nuclear reaction:

$$^{14}N_7 - ^{14}N_7 + ^{1}n_o \rightarrow ^{14}C_6 + ^{14}N_7 + ^{1}H_1 \qquad (1)$$

The carbon-14 atoms are formed with a recoil kinetic energy of about 40 keV but are rapidly thermalized by multiple collisions with other gas-phase species or the walls of the Zircaloy pressure/calandria tube system.

It is possible that the large in-core surface acts as a sink for reactive gas-phase species but S. Veprek has demonstrated that in a high energy environment capable of supporting electronically excited nitrogen or hydrogen species, surface carbon is transported in the direction of lower energy (i.e. out-of-core in this case) by the heterogeneous reactions/12,13/:

$$C(s) + N^*(g) \rightarrow CN(g) \qquad (2)$$

$$xC(s) + \frac{y}{n} H_n^*(g) \rightarrow C_xH_y(g) \qquad (3)$$

The system investigated by Veprek involved the transport of carbon in a pure nitrogen or hydrogen plasma. A polymeric material, thought to be $(CN)_n$ in nitrogen and $(C_xH_y)_n$ in hydrogen, was deposited just outside the discharge zone in each case.

For a Pickering reactor at full power there is certainly sufficient energy input to the in-core annulus gas (~ 10^9 R/hour) to allow for the conversion of thermalized carbon-14 atoms to ^{14}CN and $^{14}C_xH_y$ species either directly in the gas-phase or by the reactions (2) and (3). In addition a variety of reactive intermediates containing N, ^{14}C and H will be formed by reactions such as those given below, (or their ion-molecule counterparts),

$$N + {}^{14}CH_2 \rightarrow H{}^{14}CN + H \qquad (4)$$

$$H_2 + {}^{14}CN \rightarrow H{}^{14}CN + H \qquad (5)$$

$${}^{14}CN + H{}^{14}CN \rightarrow ({}^{14}CN)_2 + H \qquad (6)$$

$${}^{14}C_xH_y + N \rightarrow {}^{14}C_xH_{y-1}N + H \qquad (7)$$

Literature data show that reactions (4) to (7) are thermodynamically feasible and are generally very fast with rate constants in the range 10^{-10} - 10^{-13} cm^3 s^{-1}/14-17/. It is therefore evident that in a nitrogen filled annulus, nascent carbon-14 atoms are rapidly converted into simple hydrocarbons or carbon-nitrogen compounds such as hydrogen cyanide, cyanogen, cyanoacetylene, acrylonitrile, etc.

A significant aspect of the chemistry of the above species is their tendency to polymerize, especially under the influence of ionizing radiation. For example, Lind, Bardwell, and Perry/18/ investigated the radiation induced polymerization of both cyanogen and hydrogen cyanide and observed the formation of black or reddish-brown polymeric solids with empirical formulae $(CN_{0.95})_n$ and $(H_{0.97}C\ N_{0.97})_n$, respectively. Unfortunately the structures of these materials were not determined. More recently Hummel and Janssen/19/ investigated the action of Co-60 gamma-radiation on HCN and showed that the solid products which formed were essentially $(HCN)_n$ polymers with n in the range of 9 to 25. Hummel and Janssen suggested possible structures for these radiation induced polymers which are based on earlier proposals by Volker for HCN polymers formed by chemically initiated reactions/20/.

The Volker structure for the HCN polymer is, in fact, an example of a class of structures that have been proposed for other conjugated carbon-nitrogen polymers such as paracyanogen and polyacrylonitrile. It is now generally accepted that species of the type $N{\equiv}C\text{-}C \lessdot^{A}_{B}$ such as cyanogen (A, B = N), dimeric hydrogen cyanide (A=NH; B=H) or acrylonitrile ($A=CH_2$; B=H) readily undergo vinyl polymerization followed by cyclization of the nitrile groups to form so-called ladder or double-ladder polymers as shown in Figure 3.1. The double-ladder structure is particularly stable and also accounts for the unusual filamentary morphologies which have been reported for these polymers/21,22/. The initial polymerization process may be accomplished by purely thermal means but it has been reported that the cyclization reaction is promoted by traces of oxygen/23/.

Given the above facts it is proposed that the carbon-14 mesophase formed in the nitrogen-filled gas annulus systems of Pickering Units 1 and 2 is a double-ladder polymer of the type shown in Figure 3.1 except that, as alluded to above, carbonyl and/or hydroxyl groups are incorporated into the structure. It is probable that low levels of oxygen are always available in a nitrogen gas annulus due to the in-leakage of air or water. This residual oxygen will terminate carbon-nitrogen chain polymerization/cyclization reactions and thereby determine the size of the polymeric unit. It is, of course, possible that individual polymer units will subsequently link together via C-C or C-N bonds to form high molecular weight species.

If a Volker type structure/20/ is taken as a starting point and all appropriate experimental data are taken into consideration it is possible to arrive at a number of hypothetical structures for simple polymeric units in the carbon-14 mesophase; one such structure (I) is presented in Figure 3.2.

The empirical formula for structure I is $^{14}C_{20}N_{10}O_{10}H_{20}$ which results in atomic concentrations (neglecting hydrogen) of 48% carbon, 24% nitrogen and 28% oxygen. These values agree very well with the experimental values found by X-ray photoelectron spectrometry (XPS), (see Section 2.3.2), namely 52 $\pm$ 8% for carbon, 22 $\pm$ 4% for nitrogen and 26 $\pm$ 4% for oxygen. In addition the types and relative number of bonds indicated by the XPS data in Table 2.5 are consistent with structure I.

The behaviour of the carbon-14 mesophase during pyrolysis may also be accounted for by structure I. For example, moderate heating of a compound with structure I will undoubtedly yield structure II (Figure 3.2) and the volatile products $^{14}CO_2$ and NH_3. This is in full accord with the results of pyrolysis mass-spectrometry reported in Section 2.3.4. Similarly the loss of ^{14}CO and N_2, also reported in Section 2.3.4 for the high temperature pyrolysis of the carbon-14 particulate, may be envisaged through the ring-cleavage of structure II. The final product of the pyrolysis of structure I will then be structure III, tetra-aza-chrysene, a nitrogen substituted analogue of the well known polycyclic hydrocarbon chrysene, $C_{18}H_{12}$.

Thus the complete elimination of oxygen from structure I results in the loss of 30% of the carbon-14 originally present in the material. Recent investigations of samples of carbon-14 particulate have, in fact, found up to 40% activity loss by heat treatment below 400°C in reasonable agreement with expectations for structure I/24,25/.

Brief mention should also be made of the particle morphology to be expected for structure I. It was shown in Section 3.1 that the unusual morphology observed for the carbon-14 particulate material is also exhibited by a material known as carbonaceous mesophase formed by the heat treatment of polycyclic aromatic hydrocarbons. A material with structure I is clearly an ideal mesophase precursor/26/ and as such should pass through a semi-fluid (liquid crystal) phase on heating.

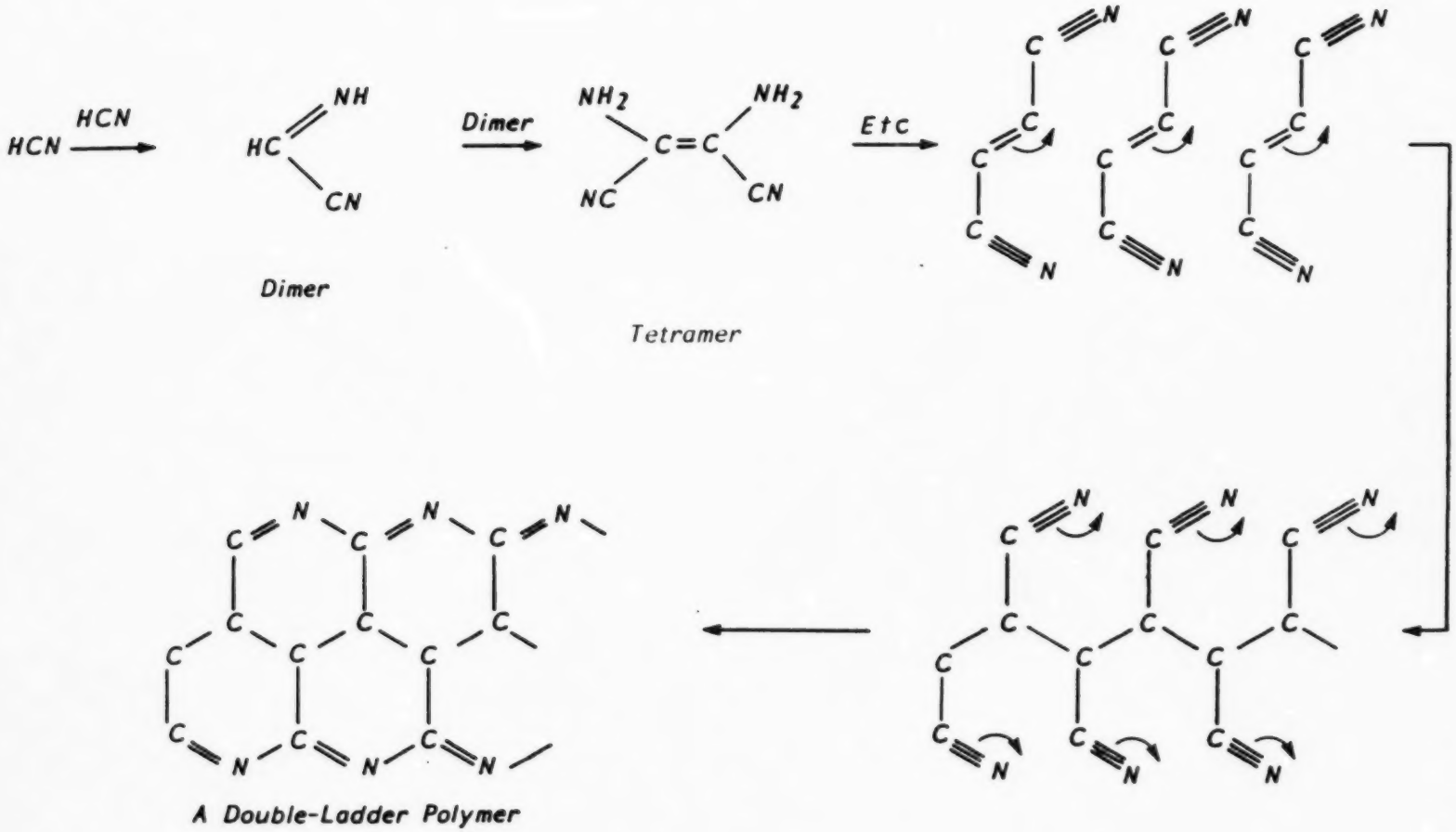

FIGURE 3.1
MECHANISM FOR THE POLYMERIZATION OF HYDROGEN CYANIDE

I.

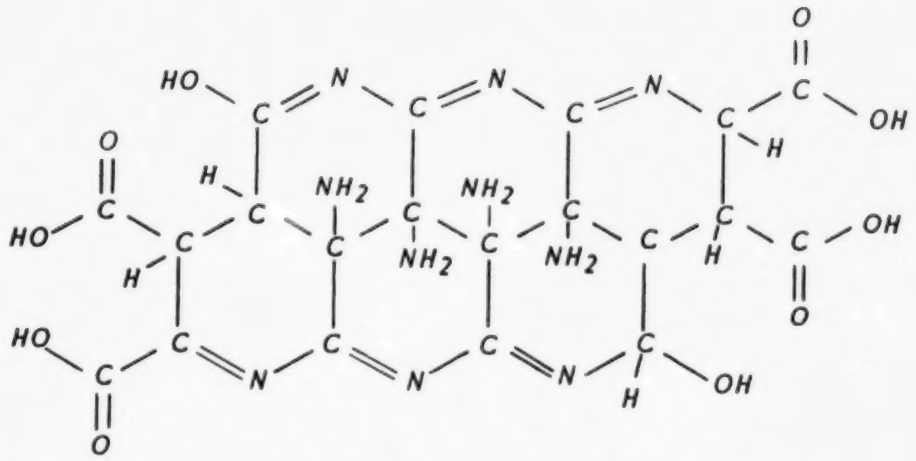

$C_{20}\ N_{10}\ O_{10}\ H_{20}$

ΔH
$-4CO_2$
$-4NH_3$

II.

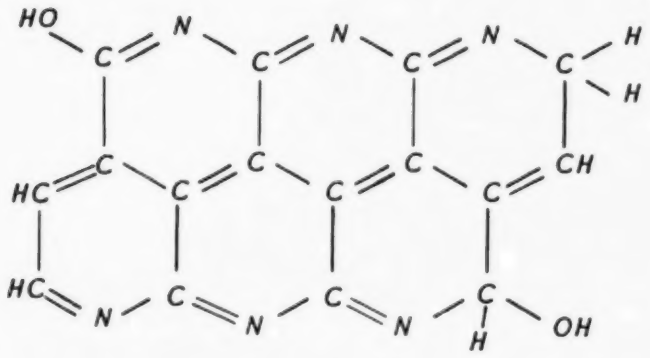

$C_{16}\ N_6\ O_2\ H_8$

ΔH
$-2CO$
$-N_2$

III.

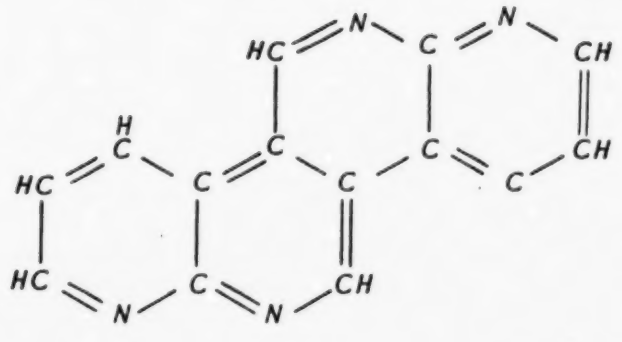

$C_{14}\ N_4\ H_8$

FIGURE 3.2

HYPOTHETICAL STRUCTURE AND PYROLYTIC BEHAVIOUR OF THE CARBON-14 MESOPHASE

Based on the micrographs included in this report it appears that most of the carbon-14 particulate receives sufficient heat treatment within the reactor core to form carbon-14 mesophase in-situ. In this case structure I may have already evolved into a highly polymerized and cross-linked form intermediate between graphite, $^{14}C_n$, and paracyanogen, $(^{14}CN)_n$, and elimination of oxygen, as $^{14}CO_2$, may then proceed during reactor operation as is known to occur. An oxygen-free carbon-14 mesophase will undergo re-uptake of oxygen on exposure to air, especially under the influence of self-radiolysis, and release $^{14}CO_2$ slowly at room temperature or rapidly on heating.

Self-radiolysis not only promotes surface oxidation of the carbon-14 mesophase, but may also induce internal changes at the molecular level. Calculations show that each β-particle released by a decaying carbon-14 atom has sufficient energy to break about 1300 bonds/11/. The fate of any displaced atoms is, of course, debatable but it is not inconceivable that they may recombine to form new structures. It is also significant that a decaying carbon-14 atom returns to a nitrogen-14 atom. It has been shown experimentally that about half of the nitrogen atoms formed by this decay process remain bound to the original molecule/27/.

About 1% of the carbon-14 originally produced in the Pickering reactors has already decayed to nitrogen and this process will continue to slowly alter the distribution of nitrogen atoms in the carbon-14 mesophase.

4.0 SUMMARY AND CONCLUSIONS

The remarkable quantity and quality (i.e. high specific activity), of the carbon-14 particulate material adhering to a tophat after insertion into and removal from a reactor supports the suggestion made in Part 1 of this report that the heaviest deposition of carbon-14 occurs at the in-board end of the lattice tube/end-fitting body in the vicinity of the split bearing sleeve. The annular gap between the inner end-fitting body and the outer lattice tube narrows at this point and presents a region of restricted flow to the annulus gas no doubt contributing to the formation of carbon-14 deposits.

Samples taken from well in-core, such as calandria or pressure tube swipes, or well out of core, such as bellows or pigtail debris, have not yielded comparable quantities of high specific activity carbon-14.

The highly active material that may be readily removed from the Unit 2 tophat is designated in this report as a carbon-14 mesophase in recognition of its resemblance to the, so-called "carbonaceous mesophase" formed during the partial graphitization of aromatic hydrocarbons.

The intriguing morphology of the carbon-14 mesophase is apparent in the micrographs reproduced in this report and presumably reflects the mode of formation of the original deposit.

Microanalysis of Unit 2 mesophase has shown it to contain about 50% carbon-14, in accordance with its high specific activity (~ 2 Ci/g), with the balance being made up of nitrogen, oxygen and hydrogen.

Vacuum pyrolysis of the mesophase liberates mainly $^{14}CO_2$ and NH_3 at low temperatures and ^{14}CO and N_2 at high temperatures. A residue, presumably ^{14}C-graphite, containing more than half of the original carbon-14 always remains after high temperature pyrolysis.

The behaviour of oxygen in the carbon-14 mesophase, e.g. its facile loss as $^{14}CO_2$, indicates that it is incorporated into the material mainly as the result of air oxidation probably after reactor shutdown. The loss of $^{14}CO_2$ (and possibly ^{14}CO) from microgram quantities of sample is detectable even at room temperature. Self-induced electron stimulated desorption may be partly responsible for this process as a consequence of the intense β-activity associated with the material.

Two specialized techniques, XPS and SIMS, have thrown some light on the functional groups present in the carbon-14 mesophase. There is good evidence for -C=N- groupings in conjugated sequences while O-N and N-N bonds may be definitely ruled out.

At the time of writing no definitive structural identification has been made for the carbon-14 mesophase. However, rather than resort entirely to descriptive, but uninformative, terms such as "an intractable polymer", a tentative structure is developed in the final pages of this report which fits very well with the observed properties of the mesophase.

The proposed structure is a nitrogen poly-heterocyclic polymer with carboxyl, hydroxyl and amino substituents; it is similar to structures that have been reported previously for HCN polymers. While this structure may appear to be somewhat exotic and its formation unlikely in the high energy conditions encountered in a nuclear reactor, the converse is, in fact, true. The spontaneous synthesis of similar species has been proposed for simple mixtures of gases in environments as diverse as interstellar space/28/, molecular gas clouds/29/, the outer planets/30/, and the atmosphere of the primitive earth/31/. That these proposals are not mere speculation is shown by the fact that simple heterocyclic compounds such as purines and pyrimidines have been identified in laboratory experiments designed to simulate the above environments/32-37/. It appears then that the formation of the carbon-14 mesophase, with its unusual nitrogen poly-heterocyclic structure, is just another example of the universal tendency of simple carbon, nitrogen and

hydrogen species to spontaneously form complex organo-nitrogen polymers in high-energy environments; in this respect it is only the intrinsic radioactivity of the carbon-14 mesophase that makes it noteworthy.

Approved by:

D.J. Dodd
Acting Manager
Chemical Research Dept

Prepared by:

F.R. Greening
Chemist
Analytical Services Section

Reviewed by:

M.R. Booth
Supervisory Chemist
Chemical Research Dept

FRG:cam

REFERENCES

1. F.R. Greening. "The Characterization of Carbon-14 Containing Particulate Material from the Gas Annulus Systems of Pickering NGS "A" Units 1 and 2", Research Division Report 86-73-K, April 1986.

2. N.S. McIntyre et al. "Studies of Vitrinitic Coal Surfaces by Ion Microscopy", Scanning Electron Microscopy/1983/III, 1115, SEM Inc., Chicago (1983).

3. D. Briggs. "SIMS for the Study of Polymer Surfaces: A Review", Surface and Interface Analysis 9, 391 (1986).

4. D. Briggs and M.P. Seah. "Practical Surface Analysis by Auger and X-Ray Photoelectron Spectroscopy", Wiley (1983).

5. C.G. Pantano and T.E. Madey. "Electron Beam Damage in Auger Electron Spectroscopy", Application of Surface Science 7, 115 (1981).

6. S.R. Heller and G.W.A. Milne. "EPA/NIH Mass Spectral Data Base", NBS, U.S. Department of Commerce (1978).

7. H. Marsh and P.L. Walker. "The Formation of Graphitizable Carbons via Mesophase: Chemical and Kinetic Considerations", Chemistry and Physics of Carbon, Vol. 15, Marcel Dekker, New York (1979).

8. H. Marsh. "Carbonization and Liquid-Crystal (Mesophase) Development: Part 1. The Significance of the Mesophase During Carbonization of Coking Coals", Fuel 52, 205 (1973).

9. H. Marsh et al. "Carbonization and Liquid-Crystal (Mesophase) Development: Part 3. Co-Carbonization of Aromatic and Heterocyclic Compounds Containing Oxygen, Nitrogen and Sulphur", Fuel 52, 243 (1973).

10. J.B. Donnet. "The Chemical Reactivity of Carbons", Carbon 6, 161 (1968).

11. P. Rochlin. "Self-Decomposition of Carbon-14-Labelled Organic Compounds", Chemical Reviews 65, 685 (1965).

12. S. Veprek. "Chemical Evaporation and Deposition of Solids in a Non-Isothermal Plasma; Chemical Transport of Carbon", Journal of Crystal Growth 17, 101 (1972).

13. S. Veprek. "Transport of Carbon in Non-Isothermal Low Pressure Nitrogen Plasma", Zeitschrift fur Physikalische Chemie Neue Folge 86, 95 (1973).

14. C. Haggart and C.A. Winkler. "The Reactions of Active Nitrogen with Cyanogen and CN Radicals", Canadian Journal of Chemistry 38, 329 (1960).

15. D.R. Safrany and W. Jaster. "Reactions of Hydrocarbons with Mixtures of Active Nitrogen and Hydrogen Atoms. II. Anomalous Reactions: The Reactions of Cyanogen, Hydrogen Cyanide, and Acetylene", Journal of Physical Chemitry 72, 3305 (1968).

16. D. Kley et al. "Observation of Carbon Atoms in Reactions of Active Nitrogen with Organic Compounds", Chemical Physics Letters 15, 45 (1972).

17. M. Berger and G.B. Kistiakowsky. "The Cyanogen-Active Nitrogen Reaction", Journal of Physical Chemistry 77, 1725 (1973).

18. S.C. Lind, D.C. Bardwell and J.H. Perry. "The Chemical Action of Gaseous Ions Produced by Alpha Particles VII. Unsaturated Carbon Compounds", Journal of the American Chemical Society 48, 1556 (1926).

19. D. Hummel and O. Janssen. "Chemishe Reaktionen der Blausaure unter der Einwirkung von ^{60}Co-γ-Strahlung", Zeitschrift fur Physikalische Chemie Neue Folge 31, 111 (1962).

20. T.H. Volker. "Polymere Blausaure", Angewandte Chemie 72, 379 (1960).

21. L.L. Bircumshaw et al. "Paracyanogen: Its Formation and Properties. Part I", Journal of the Chemical Society, 931 (1954).

22. J.H.L. Watson. "Electron Microscope Observations of the Morphology of Several Gases Polymerized by Charged-Particle Bombardment", Journal of Physical Chemistry 51, 654 (1947).

23. H.F. Mark et al (Eds). "Encyclopedia of Polymer Science and Engineering", Vol 2, p 656, Wiley Interscience (1985).

24. F.R. Greening. "The Gasification of Carbon-14 Particulate in Pickering Units 1 and 2 with Carbon-Dioxide Filled Gas Annulus Systems", Research Division Report C87-51-K, June 1987.

25. F.R. Greening. "The Gasification of Carbon-14 Particulate in Pickering Units 1 and 2 with Carbon-Dioxide Filled Gas Annulus Systems: Addendum", Research Division Report C87-62-K, July 1987.

26. I.C. Lewis and C.A. Kovac. "The Role of Free Radicals and Molecular Size in Mesophase Pitch", Carbon 16, 425 (1978).

27. V.D. Nefedov et al. "Chemical Changes During β-Decay Processes", Russian Chemical Reviews 32, 604 (1963).

28. A. Leger et al (Eds). "Polycyclic Aromatic Hydrocarbons and Astrophysics", D. Reidel Publishing (1987).

29. A. Freemand and T.J. Millar. "Formation of Complex Molecules in TMC-1", Nature 301, 402 (1983).

30. A.B. Raksit and D.K. Bohme. "Flow Tube Studies of Reactions of Cyanogen with Ions Selected From Cyanogen", International Journal of Mass Spectrometry and Ion Processes 63, 217 (1985).

31. S.W. Fox and K. Dose. "Molecular Evolution and the Origin of Life", Marcel Dekker (1972).

32. R. Hayatsu et al. "Origin of Organic Matter in the Early Solar System II. Nitrogen Compounds", Geochimica et Cosmochimica Acta 32, 175 (1968).

33. P.G. Stoks and A.W. Schwartz. "Nitrogen-Heterocyclic Compounds in Meteorites: Significance and Mechanisms of Formation", Geochimica et Cosmochimica Acta 45, 563 (1981).

34. S. Yuasa et al. "On the Abiotic Formation of Amino Acids I. HCN as a Precursor of Amino Acids Detected in Extracts of Lunar Samples", Journal of Molecular Evolution 20, 52 (1984).

35. S. Yuasa et al. "Abiotic Synthesis of Purines and Other Heterocyclic Compounds by the Action of Electrical Discharges", Journal of Molecular Evolution 21, 76 (1984).

36. B.N. Khare et al. "Organic Solids Produced by Electrical Discharge in Reducing Atmospheres: Tholin Molecular Analysis", Icarus 48, 290 (1981).

37. T. Scattergood et al. "Production of Organic Molecules in the Outer Solar System by Proton Irradiation: Laboratory Simulations", Icarus 24, 465 (1975).

DISTRIBUTION

Dr. D. Mills	Director of Research
Mr. E.S. Koehl	Pickering Health Physics
Mr. G. Armitage	Pickering SSD
Dr. G. Pilar	Pickering SSD
Mr. J. Stephenson	Pickering SSD
*Dr. B.J. Neil	Pickering SSD
Mr. G. Spielman	Pickering Operations
*Mr. E. Fracalanza	Pickering Operations
*Mr. B. Murdoch	Pickering Construction
Mr. D. Austin	Pickering Construction
*Mr. J. Morcom	Pickering Construction
*Mr. T.A. Robbins	Pickering Construction
Mr. A. Khan	Bruce Health Physics
Mr. B. Vaughan	BNPD - Services
Mr. R.T. Popple	Technical & Training Services, A02A02
Ms. J.R. Ryan	Technical & Training Services, A02C08
Dr. A Guest	Technical & Training Services, A02C07
Mr. J.T. Carrigan	Technical & Training Services
*Mr. C. Lacy	Technical & Training Services, A07F10
Mr. T. Dereski	Technical & Training Services, A07F10
Dr. D. Meranda	Design and Development - Gen, H10A12
Mr. D. Gratton	Design and Development - Gen, H11F21
Mr. R.E. Heathcock	Design and Development - Gen, H11G2
Dr. K. Woodall	Electrical Research
*Dr. J. Krasznai	Chemical Research
Mr. D. Dodd	Chemical Research
Dr. S.H. Hawthorne	Chemical Research
Mrs. S.L. Vekris	Chemical Research
Dr. F.R. Greening (3)	Chemical Research
Mrs. I. Lo (3)	Chemical Research

Public Reference Centre
Editorial Section (2)
Office Copies (3)
Extra Copies (3)

*Executive Summary Only